Received: 6 June 2019 | Revised: 19 July 2019 | Accepted: 1 August 2019

DOI: 10.1002/jmor.21054

RESEARCH ARTICLE

JOURNAL OF morphology WILEY

Developmental architecture of the nervous system in *Themiste lageniformis* (Sipuncula): New evidence from confocal laser scanning microscopy and gene expression

Allan M. Carrillo-Baltodano[1] | Michael J. Boyle[2] | Mary E. Rice[2] | Néva P. Meyer[1]

[1]Biology Department, Clark University, Worcester, Massachusetts

[2]Smithsonian Institution, Smithsonian Marine Station at Fort Pierce, Fort Pierce, Florida

Correspondence
Néva P. Meyer, Biology Department, Clark University, Worcester, MA 01610.
Email: nmeyer@clarku.edu

Funding information
American Museum of Natural History, Grant/Award Number: Lerner-Gray Fund; National Museum of Natural History, Grant/Award Number: Short-Term Visitor Award

Abstract

Sipuncula is a clade of unsegmented marine worms that are currently placed among the basal radiation of conspicuously segmented Annelida. Their new location provides a unique opportunity to reinvestigate the evolution and development of segmented body plans. Neural segmentation is clearly evident during ganglionic ventral nerve cord (VNC) formation across Sedentaria and Errantia, which includes the majority of annelids. However, recent studies show that some annelid taxa outside of Sedentaria and Errantia have a medullary cord, without ganglia, as adults. Importantly, neural development in these taxa is understudied and interpretation can vary widely. For example, reports in sipunculans range from no evidence of segmentation to vestigial segmentation as inferred from a few pairs of serially repeated neuronal cell bodies along the VNC. We investigated patterns of pan-neuronal, neuronal subtype, and axonal markers using immunohistochemistry and whole mount in situ hybridization (WMISH) during neural development in an indirect-developing sipunculan, *Themiste lageniformis*. Confocal imaging revealed two clusters of 5HT$^+$ neurons, two pairs of FMRF$^+$ neurons, and Tubulin$^+$ peripheral neurites that appear to be serially positioned along the VNC, similar to other sipunculans, to other annelids, and to spiralian taxa outside of Annelida. WMISH of a *synaptotagmin1* ortholog in *T. lageniformis* (*Tl-syt1*) showed expression throughout the centralized nervous system (CNS), including the VNC where it appears to correlate with mature 5HT$^+$ and FMRF$^+$ neurons. An ortholog of *elav1* (*Tl-elav1*) showed expression in differentiated neurons of the CNS with continuous expression in the VNC, supporting evidence of a medullary cord, and refuting evidence of ontogenetic segmentation during formation of the nervous system. Thus, we conclude that sipunculans do not exhibit any signs of morphological segmentation during development.

KEYWORDS
Annelida, elav, nervous system, Sipuncula, synaptotagmin

1 | INTRODUCTION

Across prominent spiralian groups (annelids, mollusks, flatworms, nemerteans), there is notable body-plan diversity. Despite this diversity, there are also some shared features in centralized nervous system (CNS) architecture, including an anterior brain, pairs of circumesophageal connectives, and one or more longitudinal nerve cords within developmental and adult stages (Hay-Schmidt, 2000; Hejnol & Lowe, 2015; Martín-Durán et al., 2018; Schmidt-Rhaesa, 2007). In order to determine whether such similarities reflect

Allan M. Carrillo-Baltodano and Michael J. Boyle contributed equally to this study.

 © 2019 Wiley Periodicals, Inc.

common ancestry (homology), convergence, or another evolutionary path, it is essential that we investigate the developmental formation of the CNS with a combination of modern genetic and morphological techniques in different spiralians, and at multiple life history stages. These analyses enable us to visualize characteristics during development that are otherwise undetectable through exclusive comparisons of adult morphology. In this context, the ventral nerve cord (VNC) as a component of the CNS is proving to be highly informative.

Annelids (bristle worms, earthworms, and leeches) are a spiralian taxon with segmented body plans and a predominant VNC with variable composition (Hejnol & Lowe, 2015; Müller, 2006; Purschke, Bleidorn, & Struck, 2014). Within Annelida, the ancestral nervous system was historically inferred to include a rope-ladder-like ventral cord (Bullock & Horridge, 1965; Orrhage & Müller, 2005; Purschke, 2002), with bilateral pairs of iterated ganglia joined by longitudinal connectives and transverse commissures (Richter et al., 2010). However, recent work has highlighted a diversity of neural arrangements among adult annelids, including species in some taxa with medullary cords and others with ventral cords containing intraepidermal neurons (Helm et al., 2018; Purschke, 2016; Purschke et al., 2014). And within the last decade, a series of phylogenomic studies (Andrade et al., 2015; Helm et al., 2018; Struck et al., 2011, 2015; Weigert et al., 2014; Weigert & Bleidorn, 2016) have produced new hypotheses for alternative clade arrangements, followed by subsequent ancestral character state reconstructions of annelid VNC architecture suggesting that rope-ladder-like arrangements may have evolved more than once, through convergence (Helm et al., 2018). These efforts raise an interesting possibility that evolution of the VNC within Annelida was more complicated than previously thought, and further highlights the need to explore the development of neural architecture in additional taxa.

Molecular phylogenies continue to gain support for the placement of unsegmented sipunculan worms within the overtly segmented annelids (Dordel, Fisse, Purschke, & Struck, 2010; Rousset, Pleijel, Rouse, Erséus, & Sidall, 2007; Struck et al., 2007; Zrzavý, Pavel, Piálek, & Janouškovec, 2009), and more recently, in a sister-group relationship to Errantia plus Sedentaria (Andrade et al., 2015; Helm et al., 2018; Struck et al., 2011, 2015; Weigert et al., 2014; but see Parry, Edgecombe, Eibye-jacobsen, & Vinther 2016; Parry, Tanner, & Vinther 2014; Sperling et al. 2009). Historically, phylogenetic analyses based upon comparative morphology suggested sipunculan affinities among a variety of different animal groups, including holothurians, echiurans, sternaspids, and priapulids, other echinoderms, and with annelids and/or molluscs (see Schulze et al., 2005). The Sipuncula have also been placed as the sister group to Annelida, and as a distinct metazoan phylum (Brusca & Brusca, 2003; Hyman, 1959; Stephen & Edmonds, 1972; Young, Sewell, & Rice, 2002). Different phylogenetic positions of Sipuncula using morphological characters emphasize how unique their body plan is when compared with other taxa (for reference, see Boyle & Rice, 2014), including the rest of Annelida. Challenges associated with sipunculan affinity reflect notable disagreements about the origins and definition of "segmentation" (Budd, 2001; Graham, Butts, Lumsden, & Kiecker, 2014; Hannibal & Patel, 2013; Scholtz, 2002; Seaver, 2003; Seaver & Kaneshige, 2006). Currently, genetic, developmental, and morphological characteristics of segmentation in Annelida, Arthropoda, and Chordata are not considered homologous. And repetitive structures alone have not been recognized as "true" segmentation (Budd, 2001; Scholtz, 2002; Seaver, 2003). Here, we combine definitions as presented by Scholtz (2002) and Seaver (2003) that consider an animal's body plan as segmented along the anterior–posterior axis when it is composed of repeated structural units of tissues and organ systems that develop from both ectoderm and mesoderm. Accordingly, the most recent phylogenetic position of Sipuncula makes them a pivotal group with respect to studies on the evolution and development of segmented body plans in general, and nervous systems in particular.

Previously, larval and adult sipunculan nervous systems have been described as a medullary cord, that is, an unpaired VNC lacking distinct clusters of neuronal somata and segmentally arranged commissures (Åkesson, 1958; Helm et al., 2018; Rice, 1985). However, in two sipunculan species, *Phascolosoma agassizii* and *Themiste pyroides*, Kristof, Wollesen, Maiorova, and Wanninger (2011) and Kristof, Wollesen, and Wanninger (2008) reported what they suggested were serotonergic-positive ($5HT^{+}$) "metamerically arranged perikarya" within the VNC. This pattern led the authors to suggest that during development, sipunculan nervous systems would "recapitulate" a presumed segmental organization of the last common ancestor of annelids. However, based on the hypothesis that the last common ancestor of Annelida may not have possessed a rope-ladder-like VNC (Helm et al., 2018), additional sipunculan taxa should be carefully examined to characterize the number, arrangement, and relative positions of neuronal somata, commissures, and related developmental evidence that may support or refute previous suggestions of vestigial segmentation within Sipuncula.

Here, we examined the developing nervous system in larvae and juveniles of the marine sipunculan worm *Themiste lageniformis* Baird, 1868 using cross-reactive antibodies against serotonin, Tubulin, and FMRFamide, along with in situ detection of antisense riboprobes against two neural genes, *Tl-elav1* and *Tl-syt1*. Metazoan *elav* genes encode RNA-binding proteins that are initially expressed in neuronal cells as they begin the process of differentiation, with expression maintained in mature neurons (Berger, Renner, Luer, & Technau, 2007; Pascale, Amadio, & Quattrone, 2008; Ratti et al., 2006; Robinow & White, 1991; Wakamatsu & Weston, 1997). Orthologs of *elav* have been shown to be expressed in nondividing neural cells in the annelids *Capitella teleta* (Meyer & Seaver, 2009; Sur, Magie, Seaver, & Meyer, 2017) and *Platynereis dumerilii* (Denes et al., 2007; Simionato et al., 2008). Orthologs of *synaptotagmin1* are Ca^{2+}-binding proteins that are important for exocytosis of vesicles containing neurotransmitters in the presynaptic terminals of mature neurons (Rizo & Rosenmund, 2008). Where studied, the expression of *synaptotagmin1* is initiated and maintained in mature, differentiated neurons (Denes et al., 2007; Littleton, Bellen, & Perin, 1993; Meyer, Carrillo-Baltodano, Moore, & Seaver, 2015; Nomaksteinsky et al., 2009; Santagata, Resh, Hejnol, Martindale, & Passamaneck, 2012; Simionato et al., 2008). To date, the expression patterns of neural genes have not been investigated in a member of Sipuncula. Collectively, all of the

patterns we observed, through detection of immunohistochemical markers and the expression of neural transcripts by whole-mount in situ hybridization (WMISH), provide supporting evidence for a non-ganglionated, medullary nerve cord with some iteration of cell bodies and peripheral nerves within an unsegmented sipunculan body plan. This work complements a growing body of comparative studies on nervous system development among spiralian taxa, and enables broader understanding of both taxonomic variabilities and commonalities within the developmental architecture of nervous systems across Metazoa.

2 | MATERIALS AND METHODS

2.1 | Animal collection, development, and fixation

Adult specimens of *Themiste lageniformis* Baird, 1868 were collected from oyster reefs within the Indian River Lagoon estuary near Fort Pierce, FL. On the reef, specimens were extracted from cryptic spaces among clusters of live oysters by separating them with a rock hammer, and removing the worms by hand into containers of natural seawater. In the laboratory, worms were placed in glass finger bowls of 0.35 μl filtered seawater (FSW) at room temperature (22–23 °C). Adult worms were then dissected to remove coelomic fluid containing oocytes, which were placed into gelatin-coated plastic petri dishes and cleaned with multiple exchanges of FSW, following protocols of Boyle and Seaver (2010).

Embryonic development was artificially activated by the treatment of oocytes in FSW with a final concentration of 1.0 mmol/L N,2′-*O*-dibutyryladenosine-3′:5-cyclic monophosphate (cAMP; Millipore-Sigma, St. Louis, MI, cat #D-0627). cAMP stock solution was prepared at 0.5 mol/L in dimethylformamide. cAMP activation was terminated after 1.5 hr by FSW exchanges. Embryonic and larval development was cultured in FSW with antibiotics (0.6 mg/ml penicillin; 0.5 mg/ml streptomycin) at room temperature. At designated stages of development, specimens were transferred from culture dishes to new, coated plastic petri dishes for anesthetization and fixation.

Embryonic and larval stages were anesthetized following Boyle and Seaver (2010). In brief, embryos were fixed directly in a solution of 4% paraformaldehyde (pfa) in FSW. Postgastrula and prelarval stages were relaxed with a combination of isotonic magnesium chloride ($MgCl_2$) and ethanol (EtOH, 2.5% final concentration), followed by 4% pfa fixation. Stages with active muscular contraction were relaxed with a combination of $MgCl_2$, EtOH, and 0.25% bupivacaine hydrochloride (BH; Millipore-Sigma, cat# B-5274) followed by 4% pfa. For confocal laser scanning microscopy (CLSM), fixation occurred at room temperature and was terminated within 1.0 hr by exchanges of FSW, followed by multiple exchanges and storage in phosphate-buffered saline (PBS). For WMISH (see below), fixation occurred overnight at 4.0 °C followed by termination with exchanges of FSW and PBS.

2.2 | Cloning of *Tl-elav1* and *Tl-synaptotagmin1*

Total RNA was extracted using TriReagent (Molecular Research Center, Inc., Cincinnati, OH) or an RNeasy Mini Kit (Qiagen, Hilden, Germany). cDNA was generated using the SMARTer RACE kit (Clontech, Mountain View, CA) or the Quantitect Reverse Transcription Kit (Qiagen). A *synaptotagmin 1* homolog was recovered from *T. lageniformis* by degenerate PCR using the following nested primers: forward 5′-TYAAYCCNGTNTTYAAYG and reverse 5′-TCRTTRTARTANGGRTT; second forward 5′-TAYGAYTTYGAYMG-ideoxyl-TT and second reverse 5′-SWRAARCADATRTC-ideoxyl-CC. Multiple sequences were recovered from the degenerate PCR, likely representing multiple splice variants. One 663-bp fragment (MN193560) spanning all of the C2A domain and part of the C2B domain was used to generate an antisense riboprobe. Homologs of Elav were identified from assembled transcriptomes (MJBoyle; unpublished) with Sequenceserver (Priyam et al., 2015; https://www.sequenceserver.com) from Stages 2–9 of *T. lageniformis*, blastula—pelagosphera stages in *Nephasoma pellucidum*, and 1–8 days of development in *Phascolion cryptum*, and gene orthology was assigned as detailed below. A 750-bp fragment for *Tl-elav1* (MN207127) was amplified with gene-specific primers: forward primer 5′-CGAGCAGTGAAAGCATAAAGG and reverse primer 5′-ACTAGCGGCAACAAATGAAGA. PCR fragments were cloned using either a pGEM-T easy (Promega, Madison, WI) or pCRII vector (Invitrogen) and sequenced. DIG-labeled RNA probes were generated using the MegaScript T7 transcription kit (ThermoFisher Scientific, Waltham, MA).

2.3 | Gene orthology analysis

To determine gene orthology of the *elav* genes in sipunculans, amino acid sequences for the RRM1–3 regions minus the hinge region of multiple bilaterian Elav orthologs, as well as multiple Bruno/CELF3–5 orthologs (outgroup) (Table S1), were aligned using muscle and edited by hand in MEGA7 (Figure S5). Nexus files were generated using AliView and Notepad (Microsoft, Redmond, WA). Bayesian inference was performed with the amino acid model RtRev (ProtTest3) (Darriba, Taboada, Doallo, & Posada, 2011; Guindon & Gascuel, 2003) using Mr Bayes 3.2.6 (Huelsenbeck & Ronquist, 2001). Convergence was reached after 7×10^5 generations between two simultaneous runs with sampling every 100 generations and 4 chains. A consensus tree with posterior probabilities representing 7.5×10^3 trees and a burn-in of 25% was generated in FigTree v1.4.4 (Figure S4).

2.4 | Immunostaining

Relaxation and fixation were performed as above. Depending on the stage, larvae were relaxed and fixed in either FSW or artificial sea water at room temperature, then washed several times with PBS and transferred into PBS + 0.2% Triton X-100 (PBT). Larvae were incubated in blocking solution (5% heat-inactivated goat serum [Millipore-Sigma] + PBT) for 1 hr at room temperature while rocking. Specimens were then incubated in blocking solution with the following primary antibodies: 1:500 rabbit antiserotonin (5HT; Millipore-Sigma, cat #S5545), 1:500 rabbit anti-FMRFamide (Immunostar, Hudson, WI, cat# 20091), 1:600 mouse antityrosinated Tubulin (1A-2; Millipore-Sigma, cat# T9028), and 1:10 mouse antiβ-Tubulin (E7;

Developmental Studies Hybridoma Bank, Iowa City, IA). Serotonin-like, FMRFamide-like and β-Tubulin-like immunoreactivity are designated as $5HT^+$, $FMRF^+$, and $Tubulin^+$ (Tub^+) elements throughout this manuscript. Secondary antibodies were administered in blocking solution at 1:300 goat anti-mouse $F(ab')_2$ FITC (Millipore-Sigma, cat #F8521) and 1:600 sheep anti-rabbit $F(ab')_2$ Cy3 (Millipore-Sigma, cat #C2306). DNA staining were performed by incubating the larvae in 1:1000 TO-PRO-3 (Life Technologies, Carisbad, CA, cat #T3605) in PBS according to Meyer et al. (2015) and Meyer, Boyle, Martindale, and Seaver (2010). Larvae labeled with propidium iodide (Millipore-Sigma, cat# P4864) were pretreated with RNase A (Millipore-Sigma, cat# R6513) at 1.0 mg/ml PBT for 1 hr at 37 °C, and washed with PBT before addition of primary antibodies.

2.5 | Whole-mount in situ hybridization

After fixation, specimens were dehydrated stepwise into 100% methanol and stored at −20 °C. WMISH was performed as per details in Boyle and Seaver (2010). Specimens were hybridized for 72 hr at 65 °C with 1 ng/μL of either a DIG-labeled antisense *Tl-elav1* or *Tl-synaptotagmin1* RNA probe. Probes were detected by overnight treatments of 1:5,000 anti-DIG-AP (Roche, Basel, Switzerland) at 4 °C, followed by NBT/BCIP substrate color reactions that were periodically monitored for 2–5 hr at RT. Color reactions were stopped with PBS + 0.1% Tween-20.

2.6 | Image handling and imaging

WMISH specimens were cleared and mounted in 40% glycerol (1× PBS), and imaged using DIC-optics on an AxioImager M2 compound microscope (Zeiss, Oberkochen, Germany) coupled with an 18.0 megapixel EOS Rebel T2i digital camera (Canon, Tokyo, Japan). Contrast and brightness adjustments of immunohistochemistry and WMISH images were performed in Photoshop CC and figure panels were constructed using Illustrator CC (Adobe Systems, Inc.). Z-projections were obtained from the CLSM scans using Fiji (Schindelin et al., 2012). Multiple DIC image focal planes (.TIFF) were rendered in Helicon Focus (HeliconSoft). Autofluorescent dust and precipitates near, but not touching animals, were digitally removed using Photoshop CC version 14.0 (Adobe Systems, Inc.).

Animals imaged by CLSM were dehydrated stepwise in isopropanol, and cleared and mounted in 2:1 benzyl benzoate:benzyl alcohol; or cleared and mounted in SlowFade® Gold (Life Technologies, cat# S36936). Visualization and imaging were performed with Zeiss Axioplan 2 LSM510 or Leica TCS SP5-X technology.

3 | RESULTS

3.1 | Serotonin-like ($5HT^+$) and Tubulin-like (Tub^+) immunoreactivity in *Themiste lageniformis*

A developmental staging system for *Themiste lageniformis* was previously developed by Boyle and Seaver (2010). Briefly, embryos develop via unequal spiral cleavage (Stage 1) and then gastrulate by epiboly (Stage 2) to form lecithotrophic, nonfeeding trochophore-like larvae (Stage 4). The trochophore-like larvae elongate to form nonfeeding pelagosphera larvae (Stage 8), which become competent to metamorphose into juveniles by Stage 10 (Figure 1). At Stage 5, we observed serotonergic neurons and neurites in the developing CNS (Figure 2a–d), with four pairs of $5HT^+$ neurons near the neuropil in the brain. One pair of $5HT^+$ neurons is positioned dorsal to the neuropil (dS, Figure 2d), and the other three pairs are ventral to the neuropil (vS, two pairs visible in Figure 2e). In addition to the four pairs of $5HT^+$ neurons in the brain, there is one bilateral pair of flask-shaped $5HT^+$ cells in the dorsal-most head region (fsS, Figure 2c–e). These cells each extend a single neurite to the dorsal-anterior surface of the head (Figure 2d,e). The brain connects to the VNC via paired circumesophageal connectives, which extend in a ventral-posterior direction from the brain. One pair of circumesophageal connectives is more ventral and one more dorsal (double closed arrowheads, Figure 2f). In the trunk at Stage 5, the developing VNC is visible as a concentration of cell nuclei, ranging in thickness from one to three cells, along the ventral midline (Figure 2a,c). Within the developing VNC, there are four $5HT^+$ longitudinal bundles of neurites that extend posteriorly (Figure 2a–d) toward the developing terminal organ. In the anterior VNC, there are two iterated clusters of bilaterally symmetric $5HT^+$ cells from anterior to posterior (Figure 2b,d, brackets in g). Each cluster consists of a dorsal and a ventral pair of neurons (Figure 2g), and the neurons within a cluster extend a neurite to approximately the same anterior–posterior position along the longitudinal tracts in the VNC. In addition to these two clusters of $5HT^+$ cells, there is a more posteriorly localized pair of $5HT^+$ cells (asterisks, Figure 2g) in the VNC, each of which extends a single neurite to the respective left and right longitudinal tracts of the VNC. The neurites of these posterior $5HT^+$ single neurons join the longitudinal tracts of the VNC anterior to the insertion point of the anterior-most $5HT^+$ cell cluster (Movie S1 and Figure S1). Because of the anterior insertion point for these single cells, we do not think that they are part of either of the two $5HT^+$ clusters in the VNC or are part of a presumptive third cluster that is just beginning to form. In the vicinity of the first cluster of $5HT^+$ neurons, there are peripheral neurites on each side of the trunk that extend dorsal-laterally from the VNC, and then turn anteriorly toward the head (open arrowheads, Figure 2b,d,g).

At later stages of development, we found increased $5HT^+$ immunoreactivity in the head, making it difficult to determine whether there are changes in the number of $5HT^+$ cells in the head. At Stage 6, there are still paired $5HT^+$ circumesophageal connectives and the same number and pattern of $5HT^+$ neurons in the VNC as at Stage 5 (Figure 2h–j). Changes from Stages 5 to 6 are that the $5HT^+$ longitudinal tracts of the VNC now form a "loop" just anterior to the developing terminal organ (closed arrow, Figure 2i,n, inset 2i″). Furthermore, each of the peripheral neurites associated with the first cluster of $5HT^+$ neurons extend dorsal-laterally from the VNC and now branch, with one neurite extending anteriorly toward the head, and the other neurite extending posteriorly (open arrowhead, Figure 2i,j, inset 2i′).

We also examined Tub^+ elements of the nervous system at Stage 6 (Figure 2h,j–n). Within the head, the neuropil in the brain is Tub^+. Additional Tub^+ elements include the paired circumesophageal

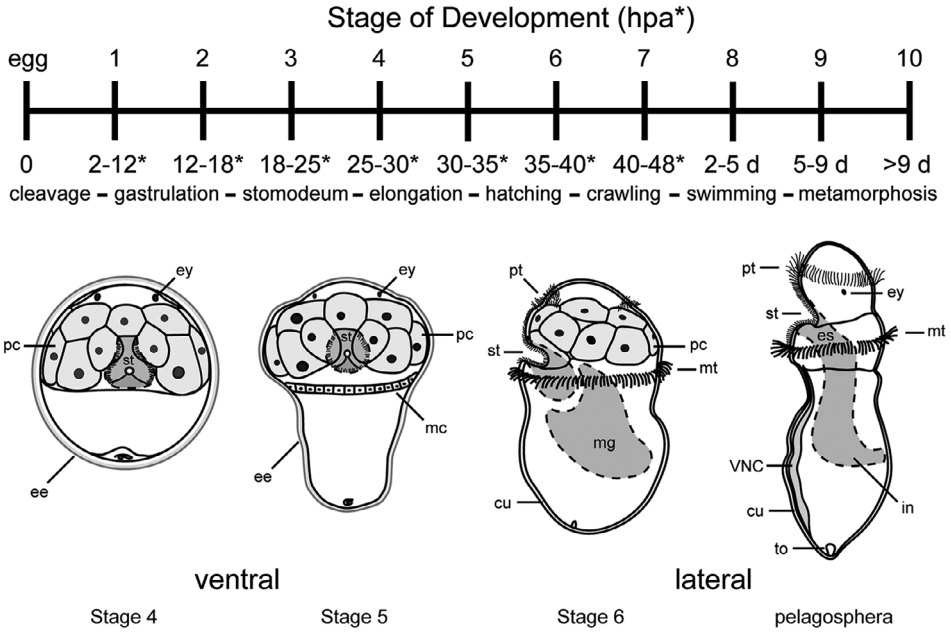

FIGURE 1 *Themiste lageniformis*, diagram of developmental stages used during this study. Development staging chart modified from Boyle and Seaver (2010), showing the stages and their corresponding ages in hours postactivation (hpa). Stages 4 and 5 are ventral views, Stage 6 and pelagosphera are lateral views with ventral to the left and anterior up. cu, cuticle; ee, egg envelope; es, esophagus; ey, eye; in, intestine; mc, metatroch cells; mg, midgut; mt, metatroch; pc, prototroch cell; pt, prototroch; st, stomodeum; to, terminal organ; VNC, ventral nerve cord

connectives and at least seven longitudinal tracts in the VNC, including the four 5HT$^+$ tracts (Figure 2h,j). There at least five Tub$^+$ transverse tracts that cross the midline in the VNC (Figure S2a–d). The transverse neurites appear to connect the left and right longitudinal tracts and are at the same dorsal-ventral position as the longitudinal tracts. The number of neurites contained within each transverse tract is unclear, but each one crosses multiple longitudinal tracts. We also detected a total of six pairs of Tub$^+$ peripheral nerves in the trunk (anterior-most pair not shown; Figure 2h,j). Interestingly, the insertion point in the VNC for four pairs of the peripheral nerves is at the same anterior-posterior position as the Tub$^+$ transverse neurites (Figure S2a–d). Five of the six pairs of peripheral nerves connect to corresponding pairs of Tub$^+$ epidermal organs or papillae in the trunk (Figure 2h, closed arrowheads in j), and these are discussed in more detail below. The second pair of peripheral nerves does not connect with papillae, but colocalizes with the 5HT$^+$ branching peripheral neurites that extend from the anterior-most 5HT$^+$ cell cluster in the VNC (compare open arrowheads in Figure 2i,j). Additional Tub$^+$ elements in the trunk include a dorsal pair of Tub$^+$ cells that are positioned between the second and third pairs of peripheral nerves near the endoderm (open arrows, Figure 2k,n). Finally, at Stage 6, the developing terminal organ at the most posterior end of the larva contains six flask-shaped Tub$^+$ cells, with three ventral and three dorsal cells (vT and dT, respectively, Figure 2l,m). Unlike the flask-shaped cells in the head, which are similar in morphology to sensory cells found in apical organs of other animals, the bulbous region of the Tub$^+$ cells in the terminal organ is apical while the narrower region is basal.

During metamorphosis from the trochophore-like stage to the pelagosphera larva (Stages 8 and 9), there are at least 10 5HT$^+$ neurons in the brain (Figure 3a–d), similar to the number observed at Stage 5. The 5HT$^+$ dorsal flask-shaped cells (fsS) are still visible and extend neurites to the dorsal-anterior surface of the head (Figure 3d). A ring of 5HT$^+$ neurites near the metatroch, which comprises cells bearing motile, compound cilia, is now visible (mtr, Figure 3b). The paired circumesophageal connectives are still 5HT$^+$ and connect to longitudinal 5HT$^+$ tracts in the VNC that are positioned closer to the ventral midline when compared to Stages 5 and 6 (Figure 3b vs. Figure 2b,i) and extend toward the terminal organ (Figure 3b,h, arrow in j). The VNC is now clearly visible by nuclear staining as a continuous band of cells (~3–5 cells deep) that run along the ventral midline (Figure 3a,f). Within the VNC, two clusters of 5HT$^+$ neurons are still present (brackets, Figure 3e); however, the number of 5HT$^+$ neurons per cluster is different than the four per cluster present at Stages 5 and 6. The first 5HT$^+$ cluster has six neurons while the second 5HT$^+$ cluster now has only two neurons (Figure 3b,e). We did not observe formation of any additional 5HT$^+$ clusters in the VNC through Day 6 of development (Figure 3b,g,i). The anterior pair of peripheral 5HT$^+$ neurites associated with the first cluster of 5HT$^+$ neurons is still present at Stages 8 and 9 and there is now a new pair of 5HT$^+$ peripheral neurites associated with the second 5HT$^+$ cell cluster (open arrowheads, Figure 3e,k). Within the first 5HT$^+$ cluster, the pair of 5HT$^+$ peripheral neurites is positioned with two neurons anterior and four neurons posterior. Finally, in the pelagosphera, there are additional 5HT$^+$ longitudinal tracts on the lateral sides of the trunk (double open arrowheads, Figure 3b,k). In contrast to the pattern of 5HT$^+$ cells in the VNC of larva, in 37-day-old juveniles, we observed an increased number of 5HT$^+$ cells scattered throughout the VNC, with no apparent clusters of 5HT$^+$ neurons (Figure S3a–c).

Within pelagosphera larvae, the larval cuticle covers the trunk, making antibody labeling difficult. In order to obtain a more distinct staining of Tub$^+$ elements in pelagosphera, we microdissected either part or all of the head to enable primary and secondary antibodies to reach the posterior end of the trunk. Using this method, we were able to visualize innervation of the epidermal papillae by the Tub$^+$ peripheral nerves (closed arrowheads, Figure 3h,i) discussed in more detail

below. At Stage 9, there are at least five Tub^{+} longitudinal tracts and at least eight transverse neurites that cross the midline (arrows pointing at five of them, Figure S2e). In juveniles, the longitudinal tracts have condensed, forming two paired longitudinal cords in the anterior half of the VNC (Figure S2f and prlt in Figure S2g) and a single, unpaired longitudinal cord in the posterior half of the VNC (Figure S2f and unlt in Figure S2h). We were not able to detect in juveniles the transverse neurites present at earlier larval stages (Figure S2f–h).

In summary, there are differentiated 5HT^{+} neurons and neurites in the brain and VNC of *T. lageniformis* starting in early larval development through juvenile stages. During larval stages, there

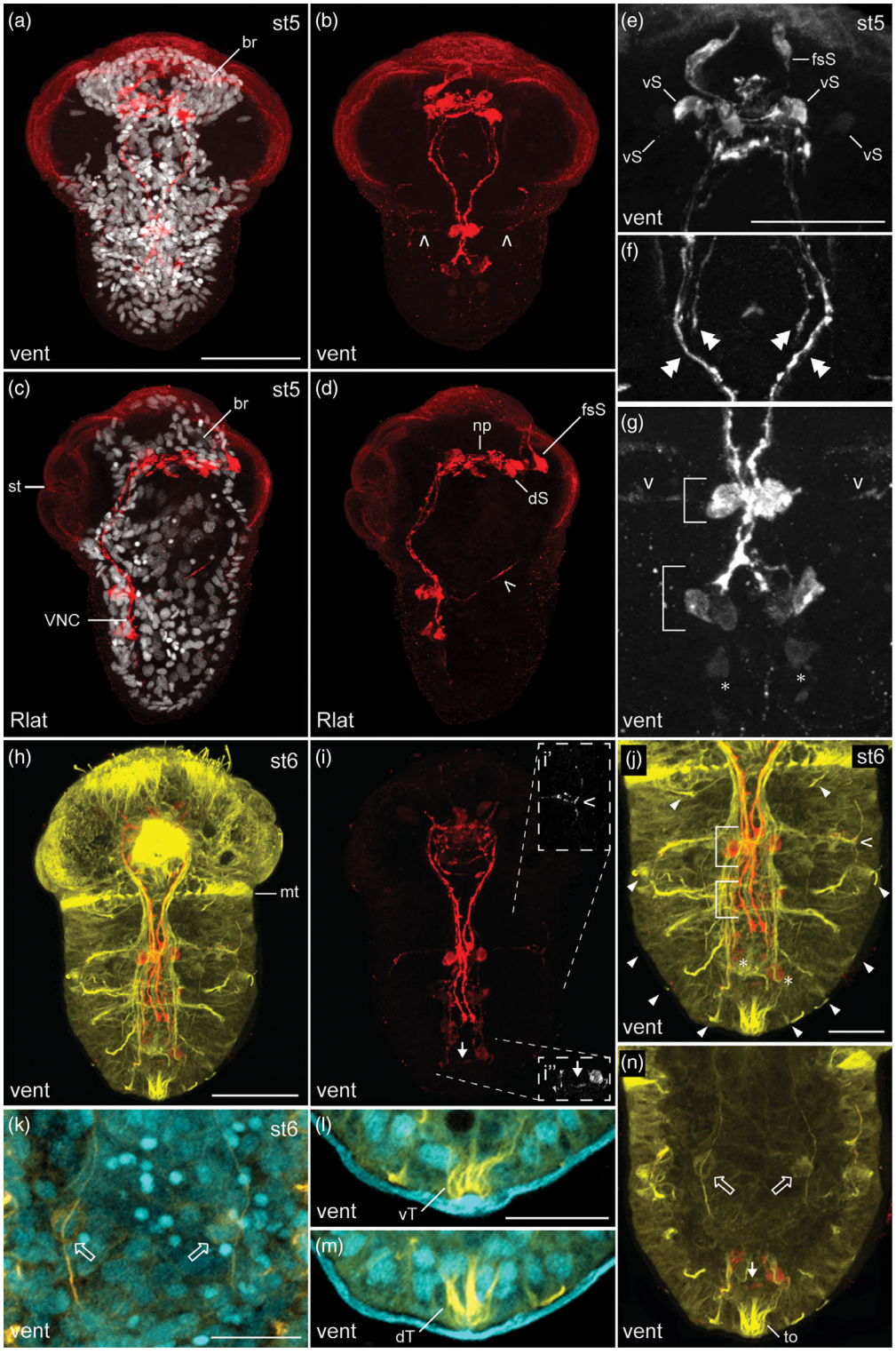

FIGURE 2 Legend on next page.

are two 5HT$^+$ clusters of neurons in the VNC with corresponding 5HT$^+$ neurites. After metamorphosis, juveniles have more 5HT$^+$ cells scattered along the A–P axis of the VNC, but the clusters of 5HT$^+$ neurons in the VNC, including the two seen in larvae, are no longer detectable.

3.2 | FMRFamidergic-like (FMRF$^+$) immunoreactivity in *Themiste lageniformis*

We used a cross-reactive, polyclonal antibody against FMRFamide to detect FMRF-like immunoreactivity (FMRF$^+$) in combination with anti-Tubulin antibodies (Tub$^+$) from Stages 5–9 in *T. lageniformis* (Figure 4). At Stage 5 in the brain, we detected two flask-shaped FMRF$^+$ cells positioned just anterior to the neuropil (fsF; one fsF shown in Figure 4b). We also detected smaller FMRF$^+$ neurons near the neuropil in the brain. At Stage 5, a pair of bilaterally symmetric, Tub$^+$ cells also are present in the most anterior region of the head (Figure 4e). From the brain, paired FMRF$^+$ circumesophageal connectives (Figure 4a, double closed arrowhead in Figure 4c) extend ventrally into the VNC where there are a pair of lateral FMRF$^+$ longitudinal tracts and a single median FMRF$^+$ longitudinal tract, none of which extend to the developing terminal organ (Figure 4a,e). Similar to the two clusters of 5HT$^+$ cells in the VNC, we found two pairs of FMRF$^+$ cells along lateral sides of the anterior half of the VNC (Figure 4a, brackets in 4d,e). Each FMRF$^+$ cell sends an axon to the longitudinal tract on their respective side of the animal, to the median longitudinal tract, and to the longitudinal tract on the opposite side of the VNC at this stage (Figure 4d). The lateral pair of FMRF$^+$ longitudinal tracts and two pairs of FMRF$^+$ cells are more laterally positioned than the 5HT$^+$ longitudinal tracts and cell clusters in the VNC. At least one peripheral FMRF$^+$ neurite on each side of the body extends laterally from just anterior to the first pair of FMRF$^+$ neurons in the VNC, and then turns dorsal-laterally toward the head (open arrowhead, Figure 4e).

At Stage 6, due to an excess of background signal we were not able to discern the pattern of FMRF$^+$ cells and neurites in the head, although in some preparations we were able to see two flask-shaped FMRF$^+$ cells, as well as two Tub$^+$ cells in the head (Figure 4g). Within the trunk, two pairs of FMRF$^+$ cells continue to be visible in the anterior half of the VNC (brackets, Figure 4f,g), but no additional FMRF$^+$ neurons were observed in the VNC at Stage 6. A lateral pair and a single median FMRF$^+$ longitudinal tract continue to be visible at Stage 6 (Figure 4f), and these extend into the posterior end of the larva in the region of the developing terminal organ. As seen at Stage 5, the peripheral FMRF$^+$ neurites extend from a position anterior to the first pair of FMRF$^+$ neurons and sweep toward the lateral-posterior before turning anteriorly (open arrowhead, Figure 4f,g).

In early pelagosphera larvae, we observed approximately five FMRF$^+$ neurons in the head, but no flask-shaped cells. In the trunk, the two lateral, two medial, and one median FMRF$^+$ longitudinal tracts in the VNC continue to be visible (Figure 4h) and now join together in a loop at the posterior end of the body, where they appear to connect with the dorsal side of the Tub$^+$ terminal organ (Figure 4h,m,n). Within the VNC, the two pairs of FMRF$^+$ neurons in the anterior half of the VNC continue to be visible (Figure 4h,n), and there are now three new medial FMRF$^+$ neurons in the posterior half of the VNC (arrows in Figure 4n and inset). In the periphery of the trunk, the anterior (first) pair of peripheral neurites (anterior pair of open arrowheads, Figure 4n) is still visible, and there are two new pairs of peripheral FMRF$^+$ neurites that now extend from each side of the VNC (second and third pairs of open arrowheads, Figure 4n). The second pair of peripheral FMRF$^+$ neurites is positioned posterior to the second pair of FMRF$^+$ cell bodies in the VNC while the third, more posterior pair of peripheral FMRF$^+$ neurites extends toward a bilaterally symmetric pair of two dorsal-lateral FMRF$^+$ neurons (open arrows, Figure 4h,n). Interestingly, these peripheral FMRF$^+$ neurons (open arrows, Figure 4i–l) end near dorsal-lateral papillae in the epidermis, but do not colocalize with papillar cells bearing external cilia (closed arrowheads, Figure 4k,l).

In summary, during early larval stages, there are two pairs of FMRF$^+$ cells and lateral longitudinal tracts in the VNC, in addition to two pairs of FMRF$^+$ peripheral neurites. Later, one more pair of FMRF$^+$ peripheral neurites and three FMRF$^+$ neurons in the posterior VNC are present.

3.3 | Peripheral nerves and the epidermal papillae in *Themiste lageniformis*

Beginning at Stage 5 through Stage 6, there are six pairs of Tub$^+$ peripheral nerves that enter/exit the VNC in the trunk, which we refer to as pairs one through six from anterior to posterior (anterior-most

FIGURE 2 *Themiste lageniformis*, 5HT$^+$ and Tub$^+$ neural elements in prelarval stages. Images are z-stack projections from confocal laser scanning micrographs of larvae labeled with anti-serotonin (red), anti-tyrosinated Tubulin (yellow), and nuclear stain (propidium iodide; grayscale) or TO-PRO3 (cyan). (a,b) Ventral and (c,d) lateral views of Stage 5 specimens showing the developing br and VNC. (e–g) Cropped and magnified images of the same animal as in (a,b), showing in (e), the fsS in the head and vS in the brain, in (f), the circumesophageal connectives (pairs of double closed arrowheads), and in (g), the two 5HT$^+$ clusters of cells (brackets) in the developing VNC and a posterior pair of 5HT$^+$ cells (asterisks). dS present in the brain are visible in (d), but not visible in (e). Transverse 5HT$^+$ peripheral neurites in the trunk are labeled with open arrowheads in (b,d) and (g). (h–n) Ventral views of a Stage 6 specimen showing the composition of 5HT$^+$ and tub$^+$ neural elements, and tub$^+$ ciliated cells. (i′) Inset showing the left transverse 5HT$^+$ neurite branching toward the anterior and posterior (open arrowhead), and (i″) a view of the 5HT$^+$ loop just anterior to the terminal organ (arrow). (j–n) Cropped magnifications of the same animal as in (h,i). Closed arrowheads in (j) point to the five pairs of Tub$^+$ papillae and brackets show the position of the two 5HT$^+$ clusters. (k,n) Deeper projections showing the two Tub$^+$ cells (open arrows). (l,m) The position of the vT and dTof the terminal organ. br, brain; dS, dorsal 5HT$^+$ cells; dT, dorsal Tub$^+$ cells of the terminal organ; fsS, flask-shaped 5HT$^+$ cells; mt, metatrochal cells; np, neuropil; st, stomodeum; to, terminal organ; VNC, ventral nerve cord; vS, ventral 5HT$^+$ cells; vT, ventral Tub$^+$ cells of the terminal organ. Scale bar is 50 μm in (a,h,j) and 25 μm in (e,k,l)

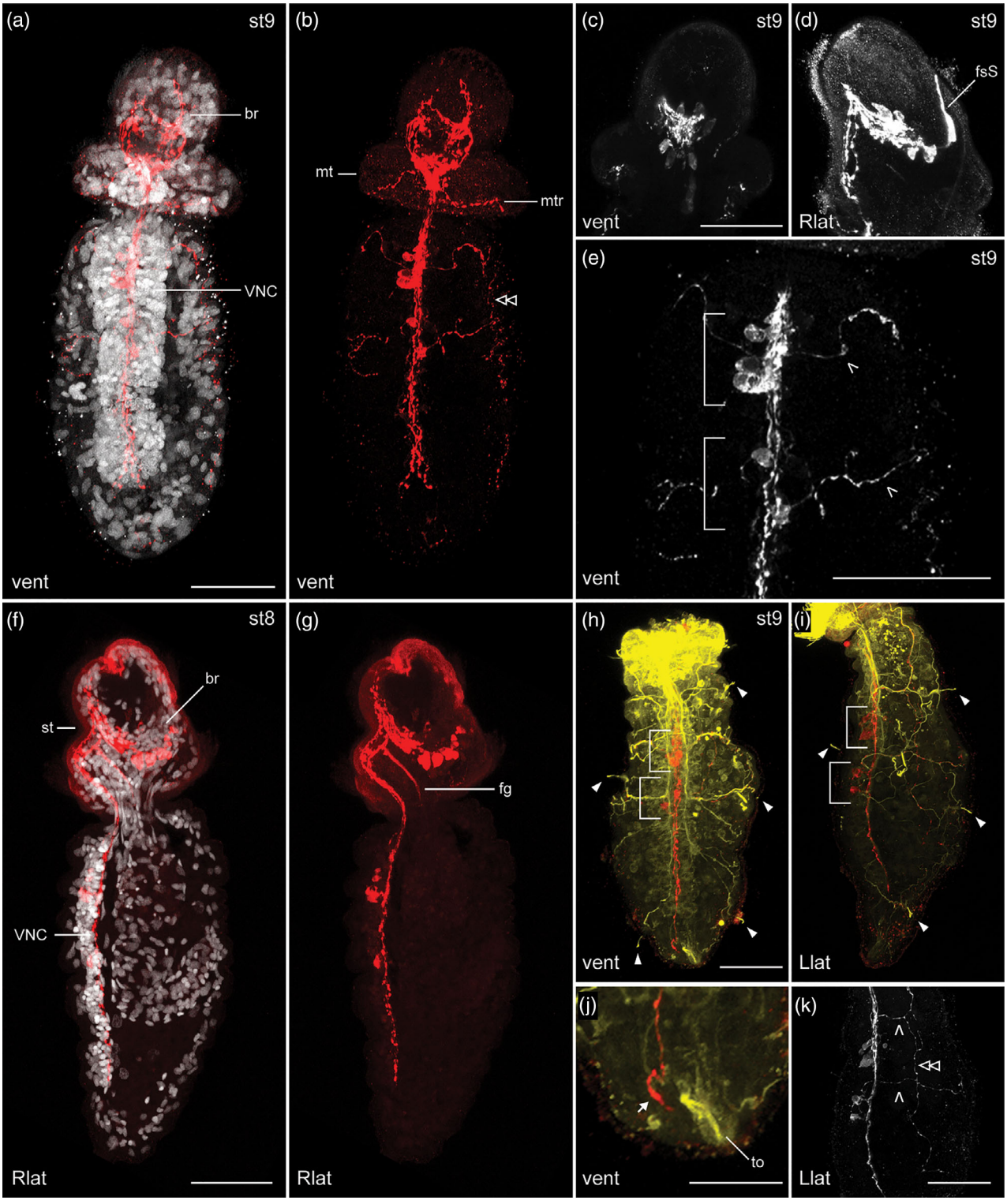

FIGURE 3 *Themiste lageniformis*, 5HT$^+$ and Tub$^+$ neural elements in the pelagosphera larva. Images are z-stack projections from confocal laser scanning micrographs of larvae labeled with anti-serotonin (red), anti-tyrosinated tubulin (yellow), and nuclear stain TO-PRO3 (grayscale). (a–c,e) Ventral and (d) lateral views of Stage 9 pelagosphera larvae showing the developing brain (br) and ventral nerve cord (VNC). (b) The metatroch (mt) and metatrochal 5HT$^+$ ring nerve (mtr) and one of the lateral 5HT$^+$ longitudinal tracts (double open arrowhead). (c) Magnified views of the brain and (e) the anterior region of the trunk from the same specimen as in (a,b). (d) Lateral magnified view of the head showing one of the pair of dorsal 5HT$^+$ flask-shaped cells. (f,g) Lateral views of a Stage 8 pelagosphera larva. (h,j) Ventral and (i,k) lateral views of a Stage 9 pelagosphera with the head removed. Brackets in (h,i) mark two 5HT$^+$ clusters, and closed arrowheads point to Tub$^+$ papillae on the surface of the trunk. These papillae are innervated by Tub$^+$ peripheral nerves. Arrow in (j) points to the posterior end of the 5HT$^+$ VNC near the terminal organ. (k) Single channel from (i) showing transverse 5HT$^+$ neurites (open arrowheads) and a lateral 5HT$^+$ longitudinal tract (double open arrowhead). br, brain; dS, dorsal 5HT$^+$ cells; fg, foregut; fsS, flask-shaped 5HT$^+$ cells; mt, metatroch; mtr, metatrochal 5HT$^+$ ring nerve; st, stomodeum; to, terminal organ; VNC, ventral nerve cord. Scale bar is 50 μm in (a,e,f,h,j,k) and 25 μm in (c)

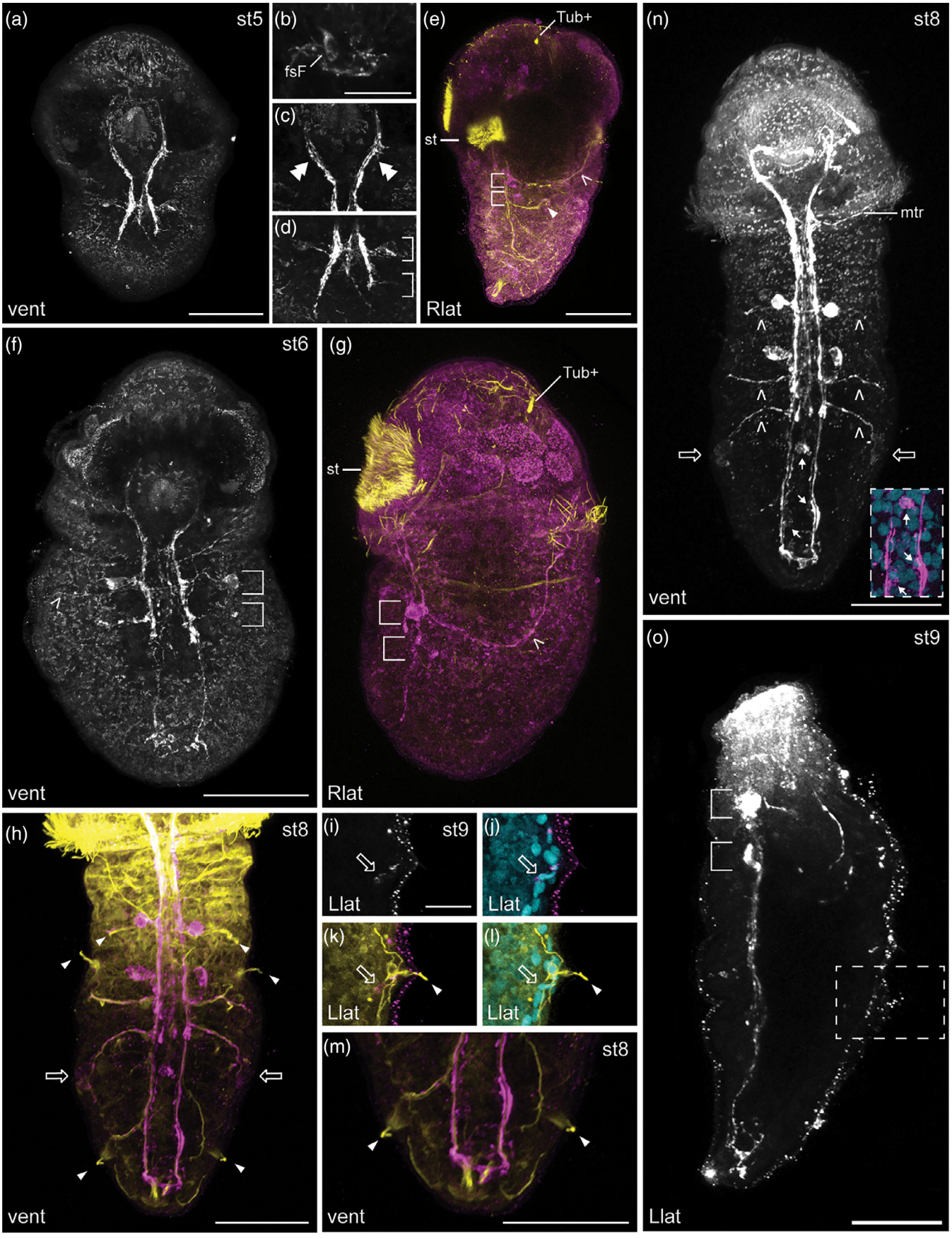

FIGURE 4 Legend on next page.

or first pair not shown; Figure 2h,j). At Stage 6, Pairs 1 and 3–6 appear to innervate five Tub$^+$ papillae at ventral, lateral, and dorsal locations throughout the epidermis in the trunk. Each papilla has one Tub$^+$ cilium that projects externally from the body (Figure 2h, closed arrowheads in j). The second pair of Tub$^+$ peripheral nerves enters/exits the VNC near the first 5HT$^+$ cluster and colabel with antibodies against 5HT and FMRF (discussed in more detail previously), but they do not appear to extend to ciliated papillae. This suggests that the second pair of Tub$^+$ peripheral nerves is different than the other pairs of Tub$^+$ peripheral nerves. The third and fourth pairs of Tub$^+$ peripheral nerves connect to the VNC at the position of the second 5HT$^+$ cluster, while the fifth and sixth pairs of Tub$^+$ peripheral nerves enter/exit the VNC at more posterior locations, and extend toward the two most posterior pairs of papillae (Figure 2h,j).

The pattern of peripheral nerves is slightly different at pelagosphera stages. There are now five instead of six pairs of Tub$^+$ peripheral nerves; the sixth pair is missing in the pelagosphera. The second pair of Tub$^+$ peripheral nerves continues to colocalize with the first pair 5HT$^+$ and FMRF$^+$ peripheral neurites; however, while the 5HT$^+$ neurites end at the 5HT$^+$ peripheral longitudinal tracts in the mid-body (Figure 3k), the second pair of Tub$^+$ neurites extends dorsally past this point and appears to innervate the second pair of papillae. Likewise, the third pair of Tub$^+$ peripheral nerves in the pelagosphera colocalizes with the second pair of peripheral 5HT$^+$ (Figure 3e) and FMRF$^+$ neurites (Figure 4h). However, neither 5HT$^+$ nor FMRF$^+$ neurites directly contact the third pair of papillae. The fourth pair of Tub$^+$ peripheral nerves colocalizes with the third pair of peripheral FMRF$^+$ neurites, which branch laterally from the VNC toward two dorsal FMRF$^+$ cells located near the fourth pair of papillae. The fourth pair of Tub$^+$ peripheral nerves, however, continues toward, and appears to innervate the ciliated papillae; whereas, the peripheral FMRF$^+$ neurites appear to be associated with papillary support cells (Figure 4i–l). Finally the fifth pair of Tub$^+$ peripheral nerves extends a little anterior to the terminal organ. Overall, from early to late larval development, there are pairs of iterated Tub$^+$ peripheral neurites that extend, in their majority, to ciliated papillae located in the epidermis. Two of these pairs of Tub$^+$ peripheral neurites colocalize with the 5HT$^+$ and FMRF$^+$ neurites and are in phase with the 5HT$^+$ clusters.

3.4 | *Tl-elav1* expression

In order to have a more comprehensive view of nervous system development in a sipunculan, we cloned orthologs of the pan-neuronal markers *elav* and *synaptotagmin1* from *T. lageniformis* (*Tl-elav1* and *Tl-syt1*) and examined their expression patterns. Previous phylogenetic analyses of Elav family members recovered two clades, one neural clade (Elav1) and one clade (Elav2), that appeared to be unique to annelids and mollusks (Meyer & Seaver, 2009; Shigeno, Parnaik, Albertin, & Ragsdale, 2015). To investigate gene orthology of these Elav proteins in sipunculans, we performed a Bayesian analysis on Elav proteins recovered from three sipunculan species, *T. lageniformis*, *N. pellucidum*, and *P. cryptum*. Similar to previous analyses, we recovered two Elav clades: one containing bilaterian neural Elav proteins (Elav1) and a separate clade (Elav2) containing Elav proteins from annelids and mollusks. All three sipunculan species had one gene that clustered in the Elav1 clade and one gene that clustered in the Elav2 clade (Figure S4). We examined expression of *Tl-elav1*, the "neural" *elav* gene.

In Stage 4, trochophore-like larvae, *Tl-elav1* is expressed in the left and right lobes of the brain (long black arrow, Figure 5a,b), including in two flask-shaped cells in the dorsal-anterior region of each lobe (fs in inset, Figure 5b). At this stage in the trunk, there also are two localized, bilaterally symmetric regions of *Tl-elav1* expression on either side of the ventral midline (long white arrow, Figure 5a,b), likely the anlage of the developing VNC. Within each of these trunk subdomains, there are at least five *Tl-elav1*$^+$ cells, all of which are subsurface (Figure 5a,b). There are also single *Tl-elav1*$^+$ cells in the posterior and dorsal-posterior regions of Stage 4 animals (closed arrowheads, Figure 5b), which may be neurons in the developing peripheral nervous system.

At Stage 5, *Tl-elav1* continues to be expressed throughout the developing brain (Figure 5c,d) and in subsurface cells in a bilaterally symmetric pattern in the trunk (long white arrow, Figure 5c,d), which likely corresponds to the developing VNC. Within each of these subdomains (left and right VNC), there are at least 10 subsurface *Tl-elav1*$^+$ cells. There are also two new regions of *Tl-elav1* expression in the trunk, one associated with the stomodeum (double arrowhead, Figure 5c,d), and one in the dorsal-posterior region (open arrowhead,

FIGURE 4 *Themiste lageniformis*, FMRF$^+$ and Tub$^+$ neural elements in Stages 5 and 6 and the pelagosphera. Images are z-stack projections from confocal laser scanning micrographs of larvae labeled with anti-FMRFamide (magenta or grayscale), anti-β-Tubulin or anti-tyrosinated Tubulin (yellow), and nuclear stain TO-PRO3 (cyan). (a) Ventral and (e) lateral views of Stage 5. (b–d) Magnified views of the same animal in (a). (b) Magnified view of the brain showing a flask-shaped FMRF$^+$ cell. (c) Double FMRF$^+$ circumesophageal connectives (double closed arrowheads). (d) Two pairs of FMRF$^+$ cells in the VNC (brackets; one pair visible). (e) Tub$^+$ cells in the head, and a FMRF$^+$ peripheral neurite extending anteriorly (open arrowhead), and a second Tub$^+$ papilla on the right side of the trunk (closed arrowhead). Brackets label the positions of the two pairs of FMRF$^+$ cells in the VNC. (f) Ventral and (g) lateral views of a Stage 6 animal showing the two pairs of FMRF$^+$ cells (brackets) in the VNC and peripheral FMRF$^+$ neurites (open arrowheads). (h,n) Ventral views of a Stage 8 pelagosphera larva showing two posterior FMRF$^+$ cells (open arrows), the second, third, and fifth pairs of Tub$^+$ papillae (closed arrowheads), and peripheral FMRF$^+$ neurites (open arrowheads). (m) Magnification of the posterior end of the same animal in (h) and (n) showing the fifth pair of Tub$^+$ papillae and the posterior FMRF$^+$ loop near the terminal organ. (o) Lateral view of a Stage 9 pelagosphera larva with two pairs of FMRF$^+$ cells in the VNC (brackets). (i–l) Close-up of the inset from (o). Open arrows in (j–l) point to one of the posterior FMRF$^+$ cells that is not colocalized with the adjacent Tub$^+$ neurite innervating the papillae (closed arrowhead). fsF, flask-shaped FMRF$^+$ cells; mtr, metatrochal FMRF$^+$ ring nerve; st, stomodeum. Scale bar is 50 μm in (a,e,f,h,m–o) and 25 μm in (b,i)

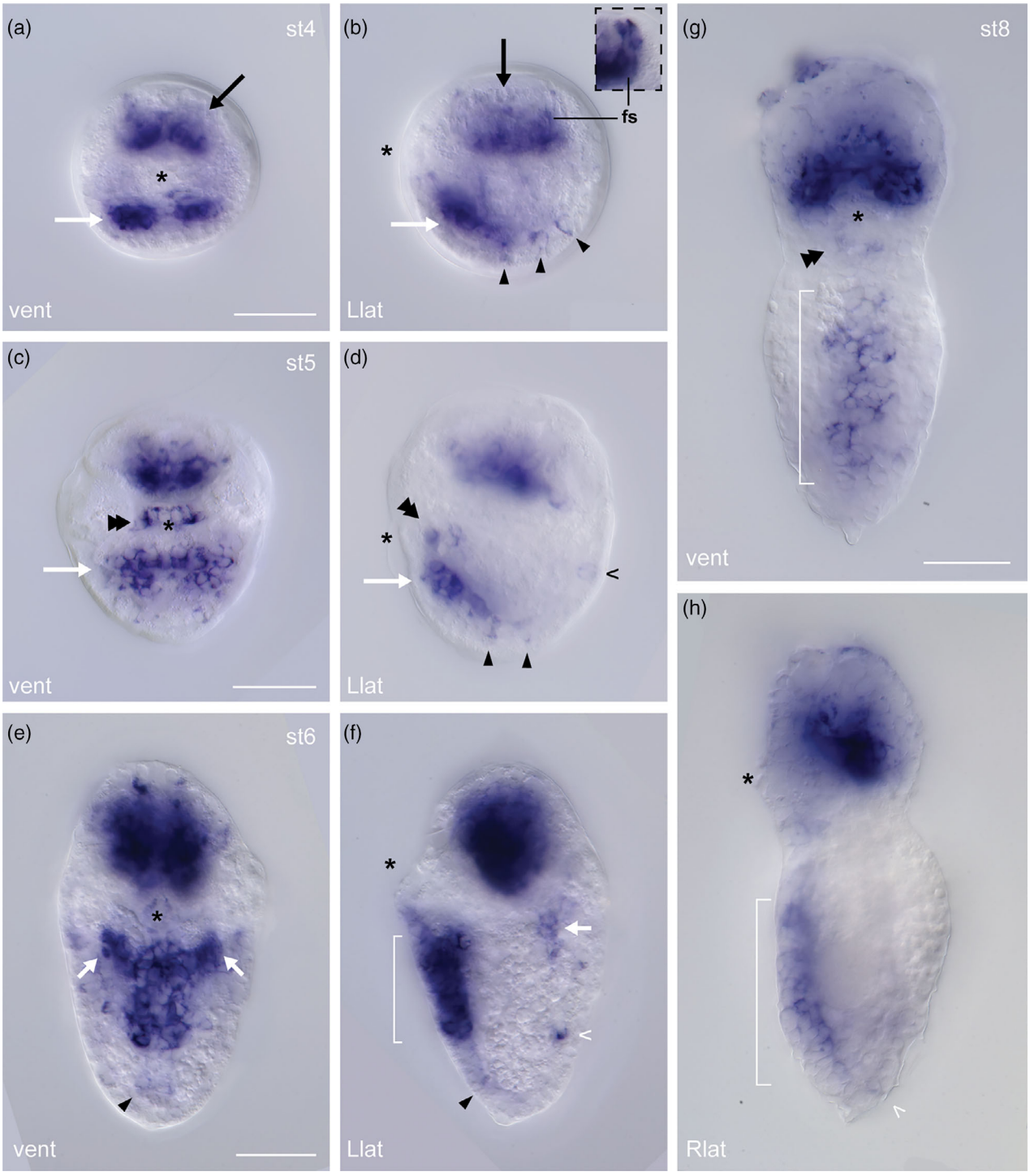

FIGURE 5 *Themiste lageniformis*, expression of *Tl-elav1* in the developing nervous system. All images are differential interference contrast (DIC) micrographs of whole-mount in situ hybridization results. (a) Ventral and (b) lateral views showing expression in the brain (black arrows) and the developing trunk (white arrows) of a trochophore-like Stage 4. Closed arrowheads in (b) point to expression in discrete cells on the dorsal-posterior side. Inset in (b) shows *Tl-elav1* expression in flask-shaped cells. (c) Ventral and (d) lateral views of Stage 5 larvae with expression in the brain and developing VNC (white arrows), and around the stomodeum (double closed arrowheads). There is at least one pair of *Tl-elav1*$^{+}$ cells on the dorsal side, opposite to the VNC (open arrowhead). (e) Ventral and (f) lateral views of Stage 6 showing bilateral expression within the developing VNC (short white arrows), and a pair of *Tl-elav1*$^{+}$ cells on the posterior end (closed arrowhead). Additionally, there is expression on the dorsal-lateral side (short white arrow), and at the expected positions of Tub^{+} papillae (open white arrowhead). (g) Ventral and (h) lateral views of a Stage 8 pelagosphera larva with *Tl-elav1* expression in a continuous sheet of cells in the region of the VNC (white bracket). Double closed arrowheads point to expression associated with the stomodeum. The open white arrowhead in (h) points at the position of another presumptive Tub^{+} papillae. Scale bar is 50 μm in (a,c,e,g). Asterisks mark the stomodeum

Figure 5d). The single *Tl-elav1*$^+$ cells in the posterior region are still present at this stage (closed arrowheads, Figure 5d).

In comparison with previous stages, at Stage 6, the two well-formed brain lobes are increased in both size and cell number and show increased levels of *Tl-elav1* expression, while the *Tl-elav1*$^+$ cells around the stomodeum were less detectable (Figure 5e,f). The developing VNC at Stage 6 is morphologically visible, and *Tl-elav1* is expressed throughout most of the VNC (Figure 5e,f). In the most anterior part of the VNC, *Tl-elav1* is expressed in bilaterally symmetric clusters of cells that extend laterally (short white arrows, Figure 5e). Within the anterior two-thirds of the VNC, expression is continuous, with no sign of "breaks" that would indicate ganglionic structures or remnants of ganglia (Figure 5e,f). In the posterior third of the VNC, *Tl-elav1* expression was less detectable; a few *Tl-elav1*$^+$ cells are indicated with a closed arrowhead in Figure 5e,f. Outside of the CNS, *Tl-elav1* is expressed in a few dorsal-lateral cells posterior to the metatroch (short white arrow, Figure 5f). At this stage, *Tl-elav1* is also expressed in two dorsal, bilaterally symmetric single cells on either side of the animal, near one of the epidermal papillae (white open arrowhead points to one *Tl-elav1*$^+$ cell near a papilla, Figure 5f).

In early pelagosphera larvae (Stage 8), *Tl-elav1* continues to be expressed in the brain (Figure 5g,h), in a few cells near the stomodeum (double arrowhead, Figure 5g), and in the VNC (brackets, Figure 5g,h). Notably, expression in the VNC appears largely continuous from anterior to posterior. Finally, *Tl-elav1* is expressed in a bilaterally symmetric pattern in a few cells on the dorsal-posterior side of the trunk, which may correspond to positions of some epidermal papillae at this stage (open arrowhead, Figure 5h). Similar to larval stages, after metamorphosis, there is continuous expression of *Tl-elav1* in the VNC (Figure S3d–f).

3.5 | *Tl-synaptotagmin1* expression

Across all stages observed, *Tl-syt1* is expressed in the developing brain and the VNC (Figure 6). This gene is also expressed near the stomodeum, and in cells throughout the ectoderm of the trunk. As observed for *Tl-elav1*, the expression of *Tl-syt1* is consistent with an expression in neurons of the central and peripheral nervous systems, including cells that may innervate the epidermal papillae and the developing terminal organ.

At Stage 4, *Tl-syt1* is expressed in both brain lobes (long black arrow, Figure 6a). There are also two patches of subsurface expression on the ventral side of the trunk (white arrows, Figure 6a,b). These two patches of expression extend transversely in "rows" across the ventral side of the embryo and correlate with a subset of the *Tl-elav1* pattern in the VNC anlage (compare Figure 6a with Figure 5a). At Stage 5, *Tl-syt1* is expressed throughout the brain and in a patch of cells posterior to the stomodeum (double arrowhead, Figure 6c,d). In the region of the developing VNC, *Tl-syt1* continues to be expressed in two transverse "rows", each of which now contains up to 10 cells (white arrows, Figure 6c,d). More posteriorly, there are *Tl-syt1*$^+$ cells along the ventral midline (open arrowhead, Figure 6c,d).

Tl-syt1 continues to be expressed in the developing brain and near the stomodeum at Stage 6 (Figure 6e,f; double-arrowhead in 6f points to expression near the stomodeum). In the VNC at Stage 6, the two transverse "rows" of *Tl-syt1* now appear as "finger-like" projections that extend laterally from a central domain of expression at the ventral midline (white arrows, Figure 6e,f). However, *Tl-syt1* is not expressed in the most posterior region of the forming VNC. *Tl-syt1* continues to be expressed in cells at the most posterior end of the trunk (open arrowhead, Figure 6e,f), near the developing terminal organ. In addition, pairs of *Tl-syt1*$^+$ cells were detected dorsally and laterally along the larval body (Figure 6e,f), and at least one of the two posterior pairs of cells is associated with a pair of epidermal papillae (closed arrowheads, Figure 6e).

At the pelagosphera stage, *Tl-syt1* continues to be expressed in the brain (Figure 6g,h), and in cells posterior to the stomodeum (double arrowhead, Figure 6g,h). As seen in earlier stages, *Tl-syt1* does not label the entire VNC, but is instead localized to the anterior half of the VNC. The two "finger-like" projections of expression in the VNC are still distinguishable (white arrows, Figure 6g,h), along with *Tl-syt1*$^+$ cells near the ventral midline (Figure 6g,h). We did not detect *Tl-syt1*$^+$ peripheral cells at this stage (Figure 6g,h). One reason for this could be that the cuticle in the trunk prevented efficient probe penetration, making visualization of single *Tl-syt*$^+$ cells in the trunk difficult.

4 | DISCUSSION

In this study, we combined immunohistochemistry and confocal microscopy with whole-mount gene expression profiles of neuronal markers to build upon and extend existing knowledge about the development of sipunculan nervous system architecture. This is the first use of all three markers (5HT$^+$, FMRF$^+$, and Tub$^+$) and neuronal genes (*Tl-elav1* and *Tl-syt1*) in any species of sipunculan marine worm. The data presented here are novel, both contrasting and complementing previous studies of sipunculan nervous systems (Åkesson, 1958; Kristof et al., 2008; Wanninger, Koop, Bromham, Noonan, & Degnan, 2005).

4.1 | Interpretation of the CNS architecture in *Themiste lageniformis*

We took a step forward from previous studies of the nervous system in sipunculans, which relied upon classical morphology and immunohistochemistry (Åkesson, 1958; Kristof et al., 2008, 2011; Wanninger et al., 2005), to study expression of pan-neuronal genes that have been shown to play a role in neuronal differentiation and maturation across Metazoa (Craxton, 2010; Pascale et al., 2008; Samson, 2008). Based on the expression of *Tl-elav1* and *Tl-syt1* in the head and the ventral trunk at Stage 4, which is shortly after gastrulation, there appear to be many differentiating and possibly mature neurons in the developing brain and VNC. We were not able to obtain information about the presence of 5HT$^+$, FMRF$^+$, and Tub$^+$ cells and neurites at Stage 4, but it is likely that these elements are already present. For example, *Tl-elav1* is expressed in two flask-shaped cells on the dorsal-

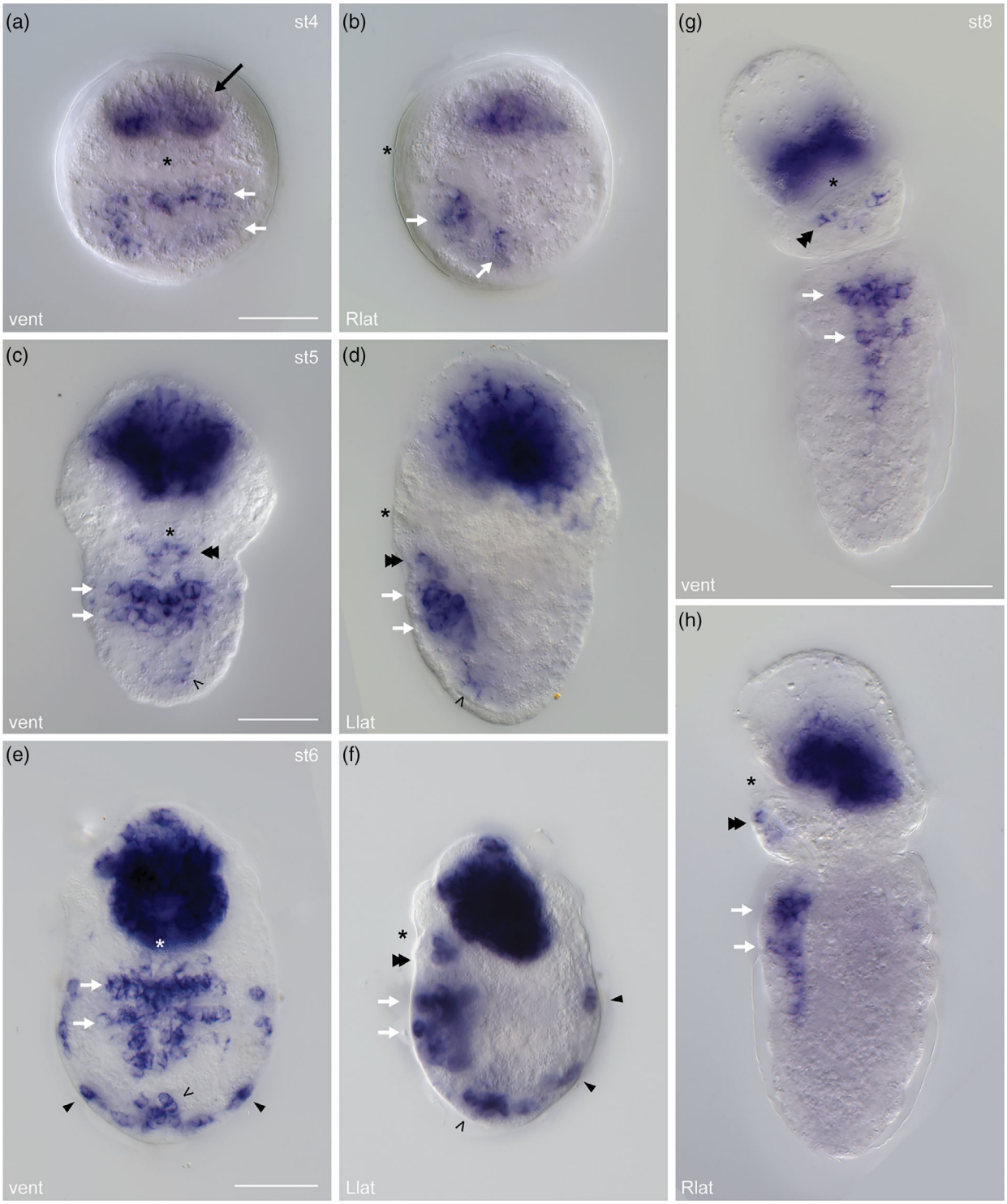

FIGURE 6 *Themiste lageniformis*, expression of *Tl-syt1* in the developing nervous system. All images are differential interference contrast (DIC) micrographs of whole-mount in situ hybridization results. (a) Ventral and (b) lateral views of Stage 4 with expression in the brain (black arrow) and as two transverse "fingers" on the ventral side within the developing trunk (short white arrows). (c) Ventral and (d) lateral views of Stage 5 showing broader expression in the brain and on the ventral side (short white arrows), in a pair of cells on the ventral-posterior end (open arrowheads), and around the stomodeum (double closed arrowheads). (e) Ventral and (f) lateral views of Stage 6 showing a more defined pattern of *Tl-syt1* expression in the brain, in transverse "fingers" across the ventral midline (short white arrows), within additional cells along the posterior region of the ventral nerve cord, in a group of cells at the posterior end (open arrowheads), and in patches of cells on left and right lateral as well as mid-dorsal sides of the trunk (closed arrowheads). (g) Ventral and (h) lateral views of a Stage 8 pelagosphera larva with transverse expression on the anterior portion of the trunk (short white arrows), but no expression on the posterior half of the ventral trunk. There is also expression in the brain and around the stomodeum at this stage (double black arrowheads). Scale bar is 50 μm in (a,c,e,g). Asterisks mark the stomodeum

anterior side of the head at Stage 4, and these are in a similar position to the flask-shaped 5HT$^+$ cells we see later at Stage 5. Moreover, the expression of *Tl-syt1* in the developing VNC matches the relative positions of the 5HT$^+$ clusters and two posterior 5HT$^+$ cells that we see later in Stage 5, as well as the pairs of FMRF$^+$ cells, providing us again with a possibility that the trochophore-like Stage 4 already has 5HT$^+$ and FMRF$^+$ cells in the trunk. Previous observations of *T. lageniformis* collected in Hawaii found at least two pairs of 5HT$^+$ cells in the trunk (NPM, unpublished data) at Stage 4, but more detailed observations at Stage 4 and earlier are needed to understand when and where the first neurons form.

The brain continues to add neurons from Stages 4–6, possibly later. There are many *Tl-elav1*$^+$ and *Tl-syt1*$^+$ cells by Stages 5 and 6 versus the ~10 5HT$^+$ and four FMRF$^+$ cells we detected (Figure 7), suggesting the presence of additional neural subtypes. The 5HT$^+$ and FMRF$^+$ cells in the brain are arranged in a bilaterally symmetric manner around a central neuropil and are connected to the VNC by paired circumesophageal connectives, which were labeled with antibodies against 5HT, FMRF, and Tubulin (Figure 7). Additional elements we detected in the brain included two dorsal flask-shaped 5HT$^+$ cells and two dorsal flask-shaped FMRF$^+$ cells, which were in close proximity to each other and may contribute to an apically positioned larval organ, similar to other apical organs present in the larvae of many other marine invertebrates (Marlow et al., 2014; Wanninger, 2008).

In the trunk, we found evidence of a nerve cord that runs along the ventral midline. At Stage 4, there are two bilaterally symmetric *Tl-elav1*$^+$ domains on either side of the ventral midline. As the larvae develop, these domains appear to converge toward the ventral midline, either by the addition of cells or by cell movement. By Stage 6, *Tl-elav1* is expressed continuously in the developing VNC from anterior to posterior and left to right. The VNC appears to be narrower from left to right at Stage 6 versus Stages 4 and 5, and this lengthening of the VNC occurs at the same time as the lengthening of the overall larval body. *Tl-elav1* continues to be expressed in the VNC from anterior to posterior in Stage 8 pelagospherae and juveniles. This, in combination with an absence of any visible "breaks" (somata-free connectives) in the nuclear stain along the VNC (e.g., Figure 3a, suggests that *T. lageniformis* does not have ganglia (concentrations of neuronal cell bodies sensu; Richter et al., 2010) in the VNC. Furthermore, there are several Tub$^+$ longitudinal tracts in the VNC by Stage 6, some of which are 5HT$^+$ and some of which are FMRF$^+$ (Figure 7). By Stages 8 and 9, the longitudinal tracts in the VNC are closer to the ventral midline than at earlier stages (Figure 7), and after metamorphosis, the tracts have condensed into two paired longitudinal cords in the anterior half of the VNC and a single, unpaired cord in the posterior half of the VNC (Figure S2f–h).

Although we did not find evidence of ganglia in the VNC during development, we did find evidence of two 5HT$^+$/FMRF$^+$ cell clusters within the VNC (Figure 7). As 5HT$^+$ and FMRF$^+$ neurons only represent a small fraction of cells in the nervous system, it would be interesting to examine a variety of neurotransmitters in *T. lageniformis* to see how other neural subtypes are arranged within the continuous tissue of the VNC. Within the developing VNC, *Tl-syt1* expression overlaps spatially with *Tl-elav1* expression. However, while *Tl-elav1* forms a continuous expression domain from Stages 5 to 8, *Tl*-syt1 is expressed in two distinct, transverse "rows" at Stages 4 and 5, and in "fingers" that extend laterally from a medial expression domain at Stages 6 and 8 (e.g., Figure 6e,g). Based on the relative positions of cells, we infer that the 5HT$^+$ clusters in the VNC are within the domains of *Tl-elav1* and *Tl-syt1* expression near the ventral midline, while the FMRF$^+$ cells in the VNC are positioned within the more lateral *Tl-syt1*$^+$ "fingers." Expression of *Tl-syt1* in two transverse bands suggests that neurons may mature in two clusters in *T. lageniformis*, which is supported by the presence of two distinct groups of 5HT$^+$ and FMRF$^+$ cells in the VNC. In addition to the presence of these two cell clusters, we also found evidence of at least five transverse bundles of neurites in the VNC, the first of which corresponds in position to the first cluster of neurons while the other bundles of transverse neurites are positioned anterior and posterior to the second cluster of neurons (Figure 7). By juvenile stages, once the longitudinal tracts have condensed, transverse neurites are no longer visible (Figure S2f–h). Furthermore, we did not observe the addition of any more clusters of 5HT$^+$ cells or additional pairs of FMRF$^+$ cells that appeared iterated along the VNC in pelagosphera larvae or juveniles. Within juveniles, distinct clusters of 5HT$^+$ cells are no longer visible, with 5HT$^+$ neurons scattered throughout the VNC. To further complicate this pattern, at Stage 9, the number of cells in the first cluster of 5HT$^+$ cells changes from four to six, and in the second cluster of 5HT$^+$ cells, from four to two, suggesting the maturation of more neurons on the anterior cluster, and possible cell death or a change in the type of neurotransmitter expressed in the second cluster. In conclusion, the developing VNC in *T. lageniformis* larvae does not exhibit a rope-ladder-like arrangement, but instead reveals a pattern of continuous neuronal somata surrounding multiple, central longitudinal neurite bundles with multiple transverse neurites. In juveniles, there are paired cords in the anterior half of the VNC and a single, unpaired cord present in the posterior half of the VNC with no detectable commissures. We find evidence of two anterior clusters of neural cell types within the continuous VNC at larval stages, but these clusters were not detectable in juveniles. Taken together, this pattern is most similar to a medullary cord (Purschke et al., 2014; Richter et al., 2010).

4.2 | Interpretation of the Peripheral Nervous System (PNS) architecture in *Themiste lageniformis*

We here provide a detailed description of peripheral nervous system formation in a sipunculan, including 5HT$^+$ neurites and FMRF$^+$ and Tub$^+$ cells and neurites. At the anterior end, we found a bilateral pair of Tub$^+$ cells located outside of the brain. These Tub$^+$ cells are similar to the bilateral Tub$^+$ cells found in larvae of *C. teleta* (sc^{ac+}) (Amiel, Henry, & Seaver, 2013; Meyer et al., 2015) and *P. dumerilii* (cPRC) (Arendt, Tessmar-raible, Snyman, Dorresteijn, & Wittbrodt, 2004; Gühmann et al., 2015), which were proved to be photoreceptor cells (Verasztó et al., 2018) in those annelids. We also found 5HT$^+$ and FMRF$^+$ neurite rings in the pelagosphera larva correlating with the

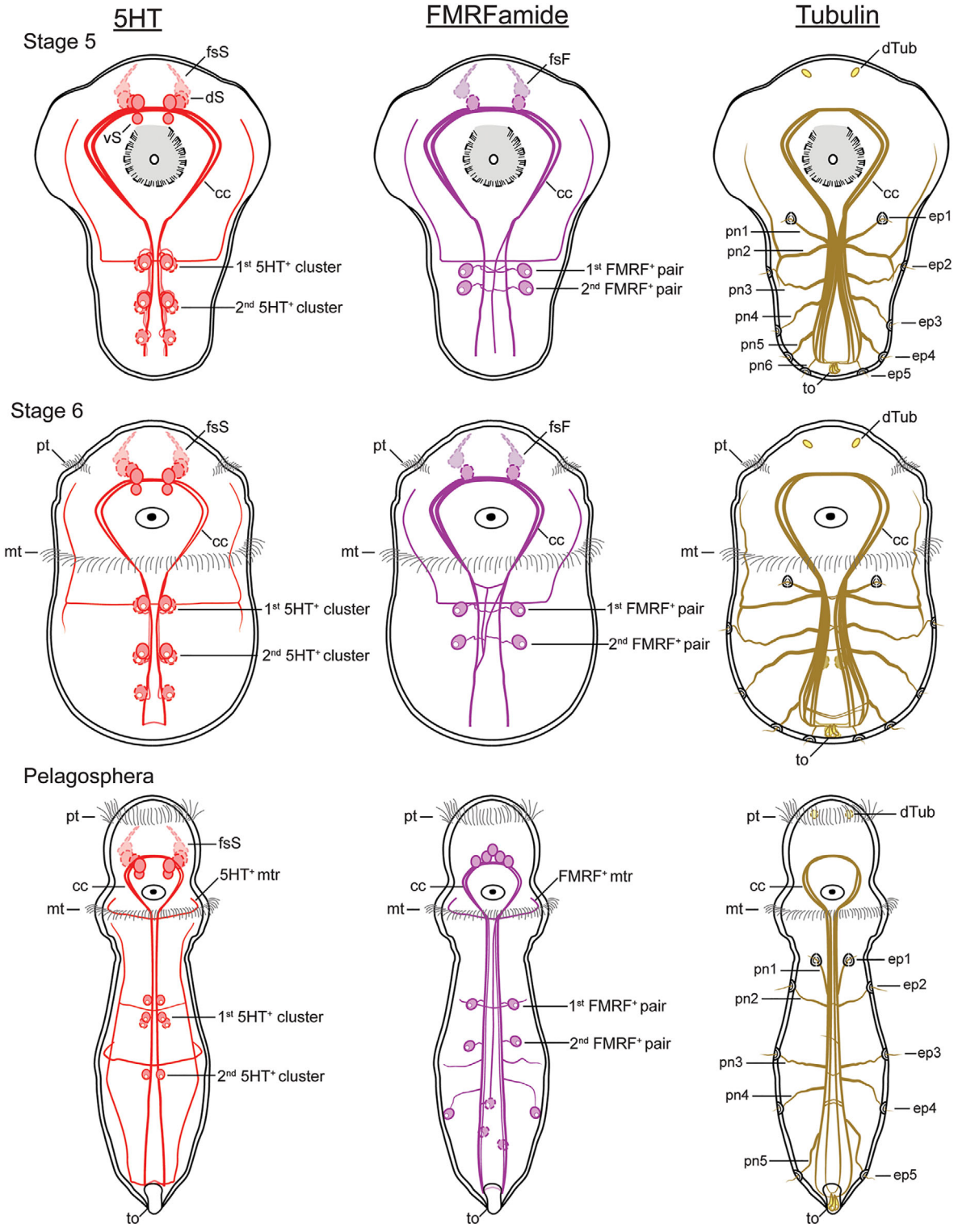

FIGURE 7 *Themiste lageniformis*, summary diagrams of the developing nervous system. $5HT^+$ (red, left), $FMRF^+$ (magenta, center), and Tub^+ (yellow, right) elements in the developing nervous system of Stages 5 and 6 and pelagosphera larvae. cc, circumesophageal connectives; dS, dorsal $5HT^+$ cells; dTub, dorsal Tub^+ cells in the head; ep1–ep5, Tub^+ epidermal papillae one through five; fsF, flask-shaped $FMRF^+$ cells; fsS, flask-shaped $5HT^+$ cells; mt, metatroch; mtr, metatrochal ring nerve; pn1–pn6, Tub^+ peripheral neurites; pt, prototroch; to, terminal organ; vS, ventral $5HT^+$ cells

metatroch, but not the prototroch, and these may be involved in controlling the beating of the cilia of the metatroch, which is the primary organ of locomotion in sipunculan pelagospherae. In *P. dumerilii*, ciliary beating of the prototroch was shown to be influenced by the presence of serotonin (Verasztó et al., 2017), which may also influence cilia in the metatroch of *T. lageniformis*. As *T. lageniformis* does not develop a ciliated prototroch, we were not able to assess whether $5HT^+$ and $FMRF^+$ neurite rings correlate with that band in sipunculan

trochophore larvae, a question that should be pursued in sipunculans with trochophore larval stages.

Within the trunk by Stage 5, there are pairs of bilaterally symmetric 5HT$^+$, FMRF$^+$, and Tub$^+$ peripheral nerves that enter/exit the VNC at the position of the first 5HT$^+$ cluster and first pair of FMRF$^+$ cells. In the pelagosphera, we detected a second pair of bilaterally symmetric 5HT$^+$, FMRF$^+$, and Tub$^+$ peripheral nerves that enter/exit the VNC from the position of the second 5HT$^+$ cluster. In addition to these peripheral nerves, we also observed Tub$^+$ nerves that enter/exit the VNC at multiple anterior–posterior locations and innervate ciliated papillae in the epidermis of the trunk, most likely providing a connection between external cues outside the body and the CNS. The Tub$^+$ neurites are arranged in an iterated pattern from anterior to posterior across all the larval stages studied. It is interesting that these neurites zig–zag laterally and reach their presumptive target (e.g., papillae), without any mesodermal septa or mesenteries that could restrict them to stereotypic branching patterns. An annelid-wide analysis with an emphasis on oligochaetes proposed that the position of ganglia is more useful than mesodermal septa to identify and describe the pattern of peripheral nerves (Zattara & Bely, 2015). Our data in *T. lageniformis* do not show any evidence of ganglia, but they do show that some of the Tub$^+$ peripheral neurites are associated with two clusters of neurons, which leads us to consider whether this pattern may suggest a putative morphological precursor for the formation of ganglia, instead of a sign of vestigial segmentation as proposed by others (Kristof et al., 2008).

4.3 | Comparison of 5HT$^+$ and FMRF$^+$ neural elements among sipunculans

Within Sipuncula, descriptions of nervous system formation using immunohistochemistry and CLSM have been published on four species: *Themiste pyroides* and *Thysanocardia nigra*, indirect lecithotrophic development with a pelagosphera larva (Kristof, 2011; Kristof et al., 2011; Kristof & Maiorova, 2016), *Phascolion strombus*, indirect lecithotrophic development without a pelagosphera (Wanninger et al., 2005), and *Phascolosoma agassizii*, indirect planktotrophic development with a pelagosphera (Kristof et al., 2008). Here, we only compare 5HT$^+$ and FMRF$^+$ neural elements between those four species and *T. lageniformis*, as no other reports of nuclear DNA or Tub$^+$ are available. Previous studies did not present replicative timelines of species–specific developmental stages. Thus, we are cautious with direct temporal comparisons of morphology and associated inferences across contrasting life history patterns.

Within trochophore and pelagosphera larval stages of *T. pyroides*, 5HT$^+$ elements include pairs of flask-shaped cells with anterior projections and other neurons associated with the neuropil of the brain, as well as paired circumesophageal connectives between the brain and VNC (Kristof, 2011; Kristof et al., 2011; Kristof & Maiorova, 2016). In "early" pelagospherae, the pattern of 5HT$^+$ cell bodies in the VNC is similar to the pattern in Stage 6 of *T. lageniformis*: two clusters of four cell bodies each, and a pair of posterior cells along paired 5HT$^+$ longitudinal tracts (Kristof et al., 2011). As observed in *T. lageniformis*, there is also a 5HT$^+$ ring-like metatrochal neurite in pelagospherae of *T. pyroides*, and one or more peripheral 5HT$^+$ neurites that extend from within the trunk toward the head (Kristof, 2011). FMRF$^+$ elements in pelagospherae of *T. pyroides* include flask-shaped cells in the brain, double circumesophageal connectives, median and lateral longitudinal tracts in the VNC, and two pairs of cells in the VNC (Kristof & Maiorova, 2016). The two pairs of FMRF$^+$ cells and longitudinal tracts are positioned laterally to 5HT$^+$ cell clusters and longitudinal tracts in the VNC (Kristof, 2011; Kristof et al., 2011; Kristof & Maiorova, 2016), similar to the pattern we observed in *T. lageniformis*, suggesting that development of the nervous system in both species is similar. Furthermore, 5HT$^+$ and FMRF$^+$ cells of the VNC in both species indicate there are two distinct groups of cell bodies along the anterior–posterior axis during VNC development in *Themiste*. Similarities between FMRF$^+$ neural elements of *T. nigra* and *T. lageniformis* include flask-shaped cells near the brain neuropil, paired circumesophageal connectives, one lateral pair and one median longitudinal tract in the VNC, and two pairs of FMRF$^+$ cells in the VNC. Additionally, one pair of FMRF$^+$ transverse neurites extends from each side of the VNC near the anterior pair of FMRF$^+$ cells, and bends in a dorsal-anterior direction toward the head (Kristof, 2011). Both pairs of FMRF$^+$ cells and longitudinal tracts are also positioned laterally to the midline in *T. nigra* (Kristof, 2011), suggesting a similar spatial relationship with corresponding 5HT$^+$ cells and longitudinal tracts in the VNC of *T. lageniformis*. No confocal data showing 5HT$^+$ elements in *T. nigra* have been published.

Phascolion strombus was the first sipunculan species in which both 5HT$^+$ and FMRF$^+$ elements were described (Wanninger et al., 2005). From their micrographs, it was not possible to determine the number or arrangement of 5HT$^+$ cells in the brain of *P. strombus*. However, the brain appears to extend single 5HT$^+$ circumesophageal connectives toward the VNC, in contrast to the paired 5HT$^+$ connectives in *Themiste*. Notably, only one cluster of 5HT$^+$ cells was detected along the developing VNC of *P. strombus*, which included an associated transverse 5HT$^+$ neurite, leading the authors to infer an absence of iteration or "cryptic" segmentation in the VNC of *P. strombus* (Wanninger et al., 2005). In contrast, they detected two pairs of FMRF$^+$ cells along the VNC, which become more apparent in early juveniles. Again, as in *Themiste* and *T. nigra*, FMRF$^+$ cell bodies and FMRF$^+$ longitudinal tracts are positioned more laterally to the midline than 5HT$^+$ neural elements (Wanninger et al., 2005). Thus, the relative positions of 5HT$^+$ and FMRF$^+$ elements along the midline appear to be a common pattern within Sipuncula.

5HT$^+$ and FMRF$^+$ elements have also been investigated in *P. agassizii*. In an "early larva," Kristof et al. (2008) detected four 5HT$^+$ cells without flask-shaped morphology in the "apical organ," and a pair of 5HT$^+$ circumesophageal connectives extending from the brain toward the developing VNC. Within the VNC, there was initially one pair of 5HT$^+$ cells, followed by development of a second pair in a "slightly older larva," With subsequent growth and elongation of the larva, they detected two more pairs of 5HT$^+$ cells, which the authors collectively interpreted as a metameric pattern of four pairs of 5HT$^+$ cells along the VNC (Kristof et al., 2008). They found one pair of FMRF$^+$ cells, and two or more FMRF$^+$ transverse peripheral neurites

branching from the VNC (Kristof et al., 2008). Based on these and other observations, Kristof et al. (2008) suggested that sequential pairs of 5HT$^+$ cells and associated "commissures" reflected anterior-to-posterior development of the rope-ladder-like VNC architecture found within Annelida. From this, they concluded that formation of the VNC in *P. agassizii*, based primarily on 5HT$^+$ elements, represented the ontogenetic recapitulation of an ancestrally segmented body plan for Sipuncula. After further comparison with *T. lageniformis* and similar studies of three other sipunculans discussed above, we do not follow that conclusion as discussed by Kristof et al. (2008). Upon closer examination of their data, we suggest that the VNC commissures may have been misidentified and that the relative anterior–posterior arrangements of 5HT$^+$ cells along the VNC may be reinterpreted as two prominent clusters, not four.

There are also histological descriptions of the developing nervous system in *Phascolion strombi*, *Gofingia minuta*, and *P. agassizii* (Åkesson, 1958; Rice, 1973). Briefly, the VNC in *P. strombi* and *G. minuta* was described to originate as a singular, unpaired median thickening of ectoderm that undergoes delamination to produce the ventral neuroblasts of an unpaired, unsegmented nerve cord (Åkesson, 1958). A similar pattern was observed by Rice (1973) during development in *P. agassizii*, although in that species, the VNC is initially paired and subsequently becomes united into a single cord within pelagosphera larvae after 2 months of growth. Interestingly, our *Tl-elav1* expression data suggest that the VNC in *T. lageniformis* forms as two bilaterally symmetric domains on either side of the ventral midline, which later becomes one continuous neural domain along the ventral midline.

Based on development of the nervous system in *T. lageniformis*, and a comparison of all sipunculan species for which similar data are published, we propose that the last common ancestor of Sipuncula had a larva possessing a medullary-like VNC with continuous neural tissue from anterior to posterior and at least two clusters of neural subtypes (including 5HT$^+$ and FMRF$^+$ neurons) in the anterior VNC. Several species of sipunculans appear to have at least two neural subtype clusters (containing both 5HT$^+$ and FMRF$^+$ neurons) at the stages examined (Kristof et al., 2008; Kristof & Maiorova, 2016; Wanninger et al., 2005), which as noted above, has been interpreted as a vestigial rope-ladder-like VNC. However, based on our data, these clusters form within a continuous field of neurons in *T. lageniformis*. We are not aware of any other reports using "pan-neuronal" markers in sipunculans, suggesting that any inference of somata-free areas in the VNC is currently problematic. Additionally, the presence or absence of VNC commissures within Sipuncula needs to be investigated in much more detail before any conclusions can be made. In *T. lageniformis*, there are Tub$^+$ tracts that are transversely oriented and cross the midline along the VNC (Figure S2). These neurites appear to connect particular left and right longitudinal tracts, although in some cases they extend peripherally from one medial bundle within the VNC toward lateral sides of the trunk body. In general, several transverse tracts are at a similar dorsal-ventral position as the longitudinal tracts. The number of neurites contained within each transverse tract is unclear; however, some do cross the longitudinal tracts. We remain cautious as to whether these transverse neurites represent definitive commissures.

In adult Sipuncula, decades of histological studies of their VNCs suggest a consistent neuroanatomical pattern, that is, the VNC comprises a ventral aggregation of cells with a dorsal core of tracts (neuropil), all of which is enclosed in a peritoneal covering of connective tissue (Bullock & Horridge, 1965; Gerould, 1938; Hilton, 1917; Rice, 1973, 1993; von Mack, 1902). Interestingly, Clark (1969) pointed out that such a distribution of neurons, being positioned ventral to the neuropil mass in Sipuncula, is in contrast to what is observed in segmented invertebrates, where the ganglionic neurons "invariably form a rind" around a centralized neuropil along the VNC. Adult VNCs in Sipuncula are subepidermally located within the coelom along the body wall of the trunk (Åkesson, 1958; Rice, 1993), with one exception. Rice (1973) noted that the cord is transiently located within the epidermal layer during early development in *P. agassizii*, which may reflect Åkesson's (1958) observations on "neuroblast delamination" prior to muscle formation in larvae. As described in *Phascolosoma* sp. by Hilton (1917) (see Bullock & Horridge, 1965), short nerves extend from the VNC to multiple attachment sites on right and left sides along the body in patterns that may be opposite, alternate, or irregular in orientation along the cord, and within the same worm. In all species examined, neuronal cell bodies appear to be evenly distributed along most of the length of the cord, with no clear evidence of ganglionic aggregations of neurons (Rice, 1993). And finally, as the histological studies briefly discussed above show, and as typically observed with most histological preparations of animals, there is a complex integration of cells, tissues, and organ systems within larval, juvenile, and adult body plans of sipunculans. It will be interesting to determine how the 5HT$^+$ and FMRF$^+$ neural elements in embryonic and larval sipunculans, especially the two clusters of neurons in the developing VNC, compare with adult neural elements, including which tissues (e.g., gut, muscle, nephridia, epidermis) they innervate.

4.4 | Comparison of VNCs in Annelida

Within the segmentally organized body plans of annelids in Errantia and Sedentaria (referred to as Pleistoannelida sensu Struck et al., 2011), the developing and adult VNC typically consists of iterated ganglia with transverse commissures along the anterior–posterior axis, somata-free connectives that connect the ganglia, and paired cords (Bullock & Horridge, 1965; Meyer et al., 2015; Müller, 2006; Orrhage & Müller, 2005; Purschke, 2002; Richter et al., 2010; Starunov, Voronezhskaya, & Nezlin, 2017; Zattara & Bely, 2015), although there are also many exceptions to this rope-ladder-like arrangement (Müller, 2006; Orrhage & Müller, 2005). This pattern is distinctly different from the unpaired medullary cord of adult sipunculans, which lack ganglia and somata-free connectives (Åkesson, 1958; Boyle & Rice, 2014; Clark, 1969; Kristof et al., 2008; Rice, 1973; Wanninger et al., 2005). However, the VNC in *T. lageniformis* shows several similarities with the VNCs of other annelids that branch outside of Errantia and Sedentaria. Current phylogenies place Oweniidae and Magelonidae as a sister clade to the rest of annelids (Andrade et al., 2015; Helm et al., 2018; Weigert et al., 2014), and the architecture of the VNC has been described in a few species in each clade (Helm, Vöcking, Kourtesis, & Hausen, 2016;

Rimskaya-Korsakova, Kristof, Malakhov, & Wanninger, 2016). Oweniids are reported to have unpaired medullary VNCs with continuous neural tissue along the ventral midline throughout the trunk (i.e., no ganglia; Helm et al., 2016, 2018; Rimskaya-Korsakova et al., 2016). However, within this unpaired cord, bilaterally symmetric, 5HT$^+$ longitudinal tracts were visible (Helm et al., 2018; Rimskaya-Korsakova et al., 2016), and in premetamorphic and postmetamorphic animals of *Owenia fusiformis*, multiple clusters of 5HT$^+$ neurons were observed in the developing VNC (Helm et al., 2016, 2018). Interestingly, in at least one oweniid species, *Myriochele heeri*, the 5HT$^+$ neurons in the VNC are uniformly distributed in the adults (Helm et al., 2018), while in another species, *Galathowenia oculata*, they are uniformly distributed in all but the most posterior segments (Rimskaya-Korsakova et al., 2016). This is similar to *T. lageniformis*, where we observed a few clusters of 5HT$^+$ and FMRF$^+$ neurons during larval stages, but a fairly uniform distribution of 5HT$^+$ neurons in juveniles. Based on these similarities, and as suggested above, we think it is possible that the cellular clusters in the developing VNC of Sipuncula either represent precursors of ganglia in this group of worms, or reflect a more general pattern across Spiralia.

In at least two species within Magelonidae, the adult VNC has also been described as medullary with irregularly arranged 5HT$^+$ and FMRF$^+$ neurons (i.e., no serial repetition). The cords are paired in the anterior and unpaired in the posterior VNC (Helm et al., 2018; Jones, 1968). The adult sipunculan VNC is unpaired based on serial cross sections (Åkesson, 1958; Rice, 1973, 1993; von Mack, 1902). This final unpaired structure is again similar to what has been described in adult oweniids, and in the posterior VNC of adult magelonids. However, in the developing VNC of sipunculan larvae, at least some of the longitudinal tracts arise as paired structures (this study; Kristof, 2011; Rice, 1973; Wanninger et al., 2005). By juvenile stages in *T. lageniformis*, these paired tracts are only visible as two closely juxtaposed Tub$^+$ cords in the anterior, while in the posterior trunk, only a single Tub$^+$ cord is visible. The paired nature of the longitudinal tracts in the VNC in larval and juvenile sipunculans could represent a developmental transition from two bilaterally symmetric domains of neural tissue on either side of the midline to the eventual single domain across the ventral midline (based on *Tl-elav1* expression). The longitudinal tracts of *T. lageniformis* and other sipunculans begin as bilaterally symmetric, but then appear to undergo fusion as development proceeds. Similarly, it is possible that different early branching annelid taxa undergo different degrees of fusion of their longitudinal tracts. It is interesting to note that all adult sipunculan species described thus far have an unpaired medullary cord (Åkesson, 1958; Rice, 1973, 1993), suggesting that the unpaired condition may be important biologically or that this feature arose early during evolution of the group, and has not undergone significant change since.

Other annelid taxa that branch outside of Sedentaria and Errantia include Chaetopteridae, Apistobranchidae, and Psammodrilidae (Helm et al., 2018), and paired medullary cords lacking somata-free connectives have been described in adult species within Chaetopteridae and Apistobranchidae (Helm et al., 2018). Within all three of these clades, the presence of serially-repeated 5HT$^+$ neuronal clusters as well as segmentally arranged commissures in the adult VNC have been described (Helm et al., 2018). Furthermore, serially repeated FMRF$^+$ neuronal clusters in the adult VNC have been described in a few species of chaetoperids and apistobranchids (Helm et al., 2018). So, while a segmented body plan is prevalent throughout Annelida except in a few groups, notably Sipuncula (Åkesson, 1958; Boyle & Rice, 2014; Clark, 1969; Wanninger et al., 2005), the presence of serially terated ganglia is not. Instead, as more taxa are being described, it appears that the rope-ladder-like VNC that has been traditionally used as a defining character for annelids (Purschke, 2002) may have evolved incrementally within different clades, that is, is not a synapomorphy of Annelida. Indeed, it has even been suggested that the rope-ladder-like architecture evolved multiple times within Annelida (Helm et al., 2018; Purschke et al., 2014). Reconstructing evolution of the VNC in annelids will require sampling across annelid groups with different morphologies, for example, with or without parapodia, sampling of groups with different life history strategies, and, importantly, sampling from early development through adult stages of the same species. If the rope-ladder-like architecture was not present in the last common ancestor of Annelida, it is interesting to speculate why clusters of neural subtypes are visible during developmental stages of at least sipunculans and oweniids, but not at later stages (i.e., juveniles or adults, respectively). This hints at the possibility that serial repetition of neural subtypes may be a developmental feature and/or a ground pattern found in other spiralian taxa. Within Annelida, what started as repetition of neural subtypes may have become codified into ganglia of rope-ladder-like VNCs in selected clades.

4.5 | Arrangement of 5HT$^+$ and FMRF$^+$ cells in the trunks of different spiralian taxa

When comparing the trunk nervous systems in larvae of other spiralians, the arrangements of 5HT$^+$ and FMRF$^+$ perikarya exhibit notable variation. In two aplacophoran larvae, there are two initial clusters of 5HT$^+$ cell bodies on each of two parallel ventral neurite bundles (Redl, Scherholz, Todt, Wollesen, & Wanninger, 2014). This pattern is relatively similar to the arrangement of 5HT$^+$ clusters along the single cord in *T. lageniformis*, although no obvious pattern of FMRF$^+$ cells in those solenogastres is detectable along the neurite bundles, unlike what we observed in *T. lageniformis*. Along parallel connectives in the ventral cord of the polyplacophoran *Ischnochiton*, 5HT$^+$ and FMRF$^+$ perikarya are more or less continuous from anterior to posterior, and do not appear to form distinct clusters (Voronezhskaya, Tyurin, & Nezlin, 2002). Within the veliger larva of a freshwater bivalve (*Dreissena polymorpha*), a pair of 5HT$^+$ ventral neurites extends between the brain and a posterior sensory cell, but no 5HT$^+$ perikarya are observed along either of the two connectives (Pavlicek, Schwaha, & Wanninger, 2018). In the veliger of the Pacific oyster (*Crassostrea gigas*), paired 5HT$^+$ and FMRF$^+$ VNCs have paired sets of perikarya that are considered pedal and visceral ganglia (Yurchenko, Yurchenko, Skiteva, Voronezhskaya, & Dyachuk, 2018). During development of a polyclad larvae, 5HT$^+$ perikarya show bilaterally symmetric patterns around a pharyngeal nerve ring, a median nerve, and dorsal-lateral connectives (Rawlinson, 2010). Compared with 5HT$^+$ cell bodies, FMRF$^+$ perikarya were not detected

along any of those neurites in the same species (Rawlinson, 2010). In the pilidium larva of *Lineus albocinctus*, FMRF$^+$ cell bodies of multipolar interneurons occur throughout a complex "nerve net" within lappet fields, while 5HT$^+$ perikarya primarily occur along lateral nerve cords, suboral neurites, and the oral nerve ring (Hindinger, Schwaha, & Wanninger, 2013). However, in the direct-developing nemertean, *Pantinonemertes californiensis*, 5HT$^+$ perikarya are continuous along each of two lateral nerve cords, and they are also found posterior to the lateral cords within a single cluster flanking the ventral midline (Hiebert & Maslakova, 2015).

Therefore, among spiralian larvae there are notable variations in the distribution and extent of 5HT$^+$ and FMRF$^+$ neural architecture. However, there is also a common developmental pattern in the way that serotonergic and FMRFamidergic nervous systems are generally wired along the anterior–posterior axis. As mentioned above, the pattern observed across larval types superficially shows an aggregation of anterior ganglia from which ventral longitudinal cords extend posteriorly. Within this pattern, 5HT$^+$ and FMRF$^+$ perikarya are typically spaced along paired nerve cords in either distinct clusters or in a linear series of cell bodies, from which neurites extend to connect them with their respective longitudinal elements (5HT$^+$ or FMRF$^+$) in the VNC. It is not clear as to what specific roles 5HT$^+$ and FMRF$^+$ perikarya have in generating different components of the CNS, or whether their particular arrangements correlate closely with functional anatomy or even body-plan organization. In segmented spiralians, 5HT$^+$ and FMRF$^+$ perikarya may align with ganglia, peripheral neurites, or appendages during early development, but then show considerable variation in later stages (Helm et al., 2016; Meyer et al., 2015; Starunov et al., 2017; Zattara & Bely, 2015). Yet, in the larvae and juveniles of unsegmented spiralians, there can also be relatively regular arrangements of 5HT$^+$ and FMRF$^+$ perikarya along the anterior–posterior axis (Friedrich, Wanninger, Brückner, & Haszprunar, 2002; Hay-Schmidt, 2000; Hiebert & Maslakova, 2015; Hindinger et al., 2013; Rawlinson, 2010; Reuter, Wikgren, & Lenthonen, 1986; Wanninger & Haszprunar, 2003). And in segmented animals outside Spiralia, 5HT$^+$ neurons can exhibit a repeated or even scattered pattern that is not correlated with segmental anatomy (Mayer & Harzsch, 2007). Thus, while observed developmental patterns of neural architecture (e.g., circumesophageal connectives, nerve cords, perikarya) may appear to correlate with or perhaps reflect the organization of some, but not all, body plans in which they are described, we suggest that 5HT$^+$ and FMRF$^+$ neural elements, although integral components of animal nervous systems, are not reliable markers of body-plan organization, especially in the context of segmented animals within Spiralia.

4.6 | Concluding remarks

Sipuncula are an ancient clade of worms with unambiguous fossil evidence of an unsegmented body plan in the Early Cambrian from ~520 million years ago (Huang, Chen, Vannier, & Saiz Salinas, 2004). Because of this, they are currently considered to represent the oldest annelid crown group (Parry et al., 2016; Weigert et al., 2014), or possibly coeval with the earliest stem group polychaetes (Parry et al., 2014). All of this brings into question the interpretations by Kristof et al. (2008), who discussed possible 5HT$^+$ evidence for the "establishment and loss" of segmentation during development of the VNC in the sipunculan, *P. agassizii*. For almost a decade, that study has been cited as the primary source of morphological evidence for the segmental ancestry of Sipuncula (Kristof et al., 2008). Our results, together with fossils pointing to the ancient history of sipunculan worms (Huang et al., 2004), suggest that such interpretations may have been premature. Clark's (1969) hypothesis that sipunculans may have diverged from an unsegmented "preannelid" lineage with a centralized nervous system, are more in line with our data on *T. lageniformis* and Helm et al. (2018).

The developmental mechanisms responsible for segmenting an animal body are not as well understood in annelids, when compared to insects or vertebrates (Chipman, 2010; Seaver, 2003). Some of the candidate "segmentation genes" such as *engrailed* and *wingless*, or pathways such as Notch signaling, have been shown as inconclusive across the few species of annelids that have been studied thus far (Gazave, Lemaı, & Balavoine, 2017; Prud'homme et al., 2003; Seaver & Kaneshige, 2006; Seaver, Paulson, Irvine, & Martindale, 2001; Seaver, Thamm, & Hill, 2005; Steinmetz, Kostyuchenko, Fischer, & Arendt, 2011; Thamm & Seaver, 2008). Only recently, teloblast cells have been found to contribute to the mesoderm of segments in the annelid *P. dumerilii* similar to the mechanisms used by clitellates (Balavoine, 2014; Özpolat, Handberg-thorsager, Vervoort, & Balavoine, 2017). It remains to be studied if this phenomenon is widespread across other annelids. Although we still are trying to understand how annelids make segments, sipunculans have been mentioned as one example of the loss of whole-body segmentation (Struck et al., 2011; Weigert et al., 2014; Weigert & Bleidorn, 2016). It has been suggested that this loss of segmentation is a result of the transition to a sedentary or "sessile" life style (Chipman, 2010); however, many clades of tubiculous polychaetes have a life style similar to sipunculans but possess a clearly segmented body plan (Rouse & Pleijel, 2001). It will be necessary to determine the molecular control of segmentation across multiple annelid taxa, both within and outside of Errantia plus Sedentaria, in order to ascertain if segmentation was either lost or had not yet evolved in the last common ancestor of Sipuncula.

In conclusion, our investigation did not uncover definitive evidence of segmental morphology during development of the sipunculan nervous system. Although we observed two clusters of perikarya, a transition from paired to unpaired longitudinal bundles, and well-supported evidence for the architecture of a medullary VNC, ancestry of a segmented body plan is not supported by patterns of common immunohistochemical markers or neuronal gene expression patterns in *T. lageniformis*.

ACKNOWLEDGMENTS

The authors wish to thank R. Bellin at the College of the Holy Cross for access to their confocal microscope, and the Smithsonian Marine Station Life Histories Program and associated support staff for assistance with field collections. AMC-B received a grant from the Lerner-Gray Fund by the American Museum of Natural History,

and NPM received a Smithsonian Short-Term Visitor award to conduct work at the Smithsonian Marine Station at Fort Pierce, Florida. This publication is Smithsonian Marine Station contribution no. 1114.

CONFLICT OF INTEREST

The authors declare no potential conflict of interest.

AUTHOR CONTRIBUTIONS

MJB, NPM, and MER designed the study. AMC-B, MJB, and NPM collected and analyzed the data. MJB and AMC-B collected the animals and provided all developmental stages. AMC-B prepared all figures, except for Figure 1. AMC-B, MJB, and NPM wrote the manuscript. All authors commented and agreed on the final version of the manuscript.

ORCID

Néva P. Meyer https://orcid.org/0000-0002-2002-3280

REFERENCES

Åkesson, B. (1958). A study of the nervous system of the Sipunculoidae, with some remarks on the development of the two species *Phascolion strombi* (Montagu) and *Golfingia minuta* (Keferstein). *Undersöksinar Over Öresund*, *38*, 1–149.

Amiel, A. R., Henry, J. Q., & Seaver, E. C. (2013). An organizing activity is required for head patterning and cell fate specification in the polychaete annelid *Capitella teleta*: New insights into cell–cell signaling in Lophotrochozoa. *Developmental Biology*, *379*(1), 107–122. https://doi.org/10.1016/j.ydbio.2013.04.011

Andrade, C. S., Novo, M., Kawauchi, G. Y., Worsaae, K., Pleijel, F., Giribet, G., & Rouse, G. W. (2015). Articulating "Archiannelids": Phylogenomics and annelid relationships, with emphasis on Meiofaunal taxa. *Molecular Biology and Evolution*, *32*(11), 2860–2875. https://doi.org/10.1093/molbev/msv157

Arendt, D., Tessmar-raible, K., Snyman, H., Dorresteijn, A. W., & Wittbrodt, J. (2004). Ciliary photoreceptors with a vertebrate-type opsin in an invertebrate brain. *Science*, *306*(5697), 869–871.

Balavoine, G. (2014). Segment formation in annelids: Patterns, processes and evolution. *International Journal of Developmental Biology*, *58*(6–8), 469–483. https://doi.org/10.1387/ijdb.140148gb

Berger, C., Renner, S., Luer, K., & Technau, G. M. (2007). The commonly used marker ELAV is transiently expressed in neuroblasts and glial cells in the *Drosophila* embryonic CNS. *Developmental Dynamics*, *236*, 3562–3568.

Boyle, M. J., & Rice, M. E. (2014). Sipuncula: An emerging model of spiralian development and evolution. *International Journal of Developmental Biology*, *58*(6–8), 485–499. https://doi.org/10.1387/ijdb.140095mb

Boyle, M. J., & Seaver, E. C. (2010). Expression of *FoxA* and *GATA* transcription factors correlates with regionalized gut development in two lophotrochozoan marine worms: *Chaetopterus* (Annelida) and *Themiste lageniformis* (Sipuncula). *EvoDevo*, *1*(1), 2. https://doi.org/10.1186/2041-9139-1-2

Brusca, R. C., & Brusca, G. J. (2003). *Invertebrates* (2nd ed.). Sunderland, MA: Sinauer Associates, Inc.

Budd, G. E. (2001). Why are arthropods segmented? *Evolution & Development*, *3*(5), 332–342. https://doi.org/10.1046/j.1525-142X.2001.01041.x

Bullock, T. H., & Horridge, G. A. (1965). *Structure and function in the nervous systems of invertebrates*. New York, NY: Freeman & Company.

Chipman, A. D. (2010). Parallel evolution of segmentation by co-option of ancestral gene regulatory networks. *BioEssays*, *32*(1), 60–70. https://doi.org/10.1002/bies.200900130

Clark, R. B. (1969). Systematics and phylogeny: Annelida, Echiura, Sipuncula. In M. Florkin & B. T. Scheer (Eds.), *Chemical zoology volume 4* (pp. 1–68). New York, NY: Academic Press.

Craxton, M. (2010). A manual collection of *Syt*, *Esyt*, *Rph3a*, *Rph3al*, *Doc2*, and *Dblc2* genes from 46 metazoan genomes—An open access resource for neuroscience and evolutionary biology. *BMC Genomics*, *11*, 37. https://doi.org/10.1186/1471-2164-11-37

Darriba, D., Taboada, G. L., Doallo, R., & Posada, D. (2011). ProtTest 3: Fast selection of best-fit models of protein evolution. *Bioinformatics*, *27*(8), 1164–1165.

Denes, A. S., Jékely, G., Steinmetz, P. R. H., Raible, F., Snyman, H., Prud'homme, B., … Arendt, D. (2007). Molecular architecture of annelid nerve cord supports common origin of nervous system centralization in bilateria. *Cell*, *129*(2), 277–288. https://doi.org/10.1016/j.cell.2007.02.040

Dordel, J., Fisse, F., Purschke, G., & Struck, T. H. (2010). Phylogenetic position of Sipuncula derived from multi-gene and phylogenomic data and its implication for the evolution of segmentation. *Journal of Zoological Systematics and Evolutionary Research*, *48*, 197–207. https://doi.org/10.1111/j.1439-0469.2010.00567.x

Friedrich, S., Wanninger, A., Brückner, M., & Haszprunar, G. (2002). Neurogenesis in the mossy chiton, *Mopalia muscosa* (Gould) (Polyplacophora): Evidence against molluscan metamerism. *Journal of Morphology*, *253*, 109–117. https://doi.org/10.1002/jmor.10010

Gazave, E., Lemaı, Q. I. B., & Balavoine, G. (2017). The notch pathway in the annelid *Platynereis*: Insights into chaetogenesis and neurogenesis processes. *Open Biology*, *7*, 160242.

Gerould, J. H. (1938). Eyes and nervous system of *Phascolosoma verillii* and other sipunculids. *Travaux de La Station Zoologique de Wimereux*, *13*, 313–325.

Graham, A., Butts, T., Lumsden, A., & Kiecker, C. (2014). What can vertebrates tell us about segmentation? *EvoDevo*, *5*(1), 24. https://doi.org/10.1186/2041-9139-5-24

Gühmann, M., Jia, H., Randel, N., Verasztó, C., Bezares-Calderón, L. A., Michiels, N. K., … Jékely, G. (2015). Spectral tuning of phototaxis by a Go-Opsin in the rhabdomeric eyes of *Platynereis*. *Current Biology*, *25*(17), 2265–2271. https://doi.org/10.1016/j.cub.2015.07.017

Guindon, S., & Gascuel, O. (2003). A simple, fast, and accurate algorithm to estimate large phylogenies by maximum likelihood. *Systematic Biology*, *52*(5), 696–704.

Hannibal, R. L., & Patel, N. H. (2013). What is a segment? *EvoDevo*, *4*(1), 35. https://doi.org/10.1186/2041-9139-4-35

Hay-Schmidt, A. (2000). The evolution of the serotonergic nervous system. *Proceedings of the Royal Society. Biological Sciences*, *267*(1448), 1071–1079. https://doi.org/10.1098/rspb.2000.1111

Hejnol, A., & Lowe, C. J. (2015). Embracing the comparative approach: How robust phylogenies and broader developmental sampling impacts the understanding of nervous system evolution. *Philosophical Transactions of the Royal Society of London. Series B, Biological Sciences*, *370*, 20150045.

Helm, C., Beckers, P., Bartolomaeus, T., Drukewitz, S. H., Kourtesis, I., Weigert, A., … Bleidorn, C. (2018). Convergent evolution of the ladder-like ventral nerve cord in Annelida. *Frontiers in Zoology*, *15*(36), 1–17.

Helm, C., Vöcking, O., Kourtesis, I., & Hausen, H. (2016). *Owenia fusiformis*—A basally branching annelid suitable for studying ancestral features of annelid neural development. *BMC Evolutionary Biology*, *16*(129), 1–19. https://doi.org/10.1186/s12862-016-0690-4

Hiebert, L. S., & Maslakova, S. A. (2015). Expression of *Hox*, *Cdx*, and *Six3/6* genes in the hoplonemertean *Pantinonemertes californiensis* offers insight into the evolution of maximally indirect development in

the phylum Nemertea. *EvoDevo*, *6*(26), 1–15. https://doi.org/10.1186/s13227-015-0021-7

Hilton, W. A. (1917). The central nervous system of a sipunculid. *Journal of Entomology and Zoology*, *9*(1), 30–33.

Hindinger, S., Schwaha, T., & Wanninger, A. (2013). Immunocytochemical studies reveal novel neural structures in nemertean pilidium larvae and provide evidence for incorporation of larval components into the juvenile nervous system. *Frontiers in Zoology*, *10*(1), 31. https://doi.org/10.1186/1742-9994-10-31

Huang, D.-Y., Chen, J.-Y., Vannier, J., & Saiz Salinas, J. I. (2004). Early Cambrian sipunculan worms from Southwest China early Cambrian sipunculan worms from Southwest China. *Proceedings of the Royal Society B Biological Sciences*, *271*, 1671–1676. https://doi.org/10.1098/rspb.2004.2774

Huelsenbeck, J. P., & Ronquist, F. (2001). MRBAYES: Bayesian inference of phylogenetic trees. *Bioinformatics*, *17*(8), 754–755.

Hyman, L. H. (1959). Phylum Sipuncula. In *The invertebrates. Vol.5: Smaller coelomate groups* (pp. 610–690). New York, NY: McGraw-Hill.

Jones, M. L. (1968). On the morphology, feeding, and behavior of *Magelona* sp. *Biological Bulletin*, *134*(272–297), 272–297.

Kristof, A. (2011). *The molecular and developmental basis of bodyplan patterning in Sipuncula and the evolution of segmentation*, Copenhagen, Denmark: University of Copenhagen.

Kristof, A., & Maiorova, A. S. (2016). 23. Annelida: Sipuncula. In A. Schmidt-Rhaesa, S. Harzsch, & G. Purschke (Eds.), *Structure and evolution of invertebrate nervous systems* (pp. 248–253). Oxford, England: Oxford University Press.

Kristof, A., Wollesen, T., Maiorova, A. S., & Wanninger, A. (2011). Cellular and muscular growth patterns during sipunculan development. *Journal of Experimental Zoology. Part B, Molecular and Developmental Evolution*, *316B*(3), 227–240. https://doi.org/10.1002/jez.b.21394

Kristof, A., Wollesen, T., & Wanninger, A. (2008). Segmental mode of neural patterning in sipuncula. *Current Biology*, *18*(15), 1129–1132. https://doi.org/10.1016/j.cub.2008.06.066

Littleton, J. T., Bellen, H. J., & Perin, M. S. (1993). Expression of *synaptotagmin* in *Drosophila* reveals transport and localization of synaptic vesicles to the synapse. *Development (Cambridge, England)*, *118*(4), 1077–1088. Retrieved from. http://www.ncbi.nlm.nih.gov/pubmed/8269841

Marlow, H., Tosches, M. A., Tomer, R., Steinmetz, P. R., Lauri, A., Larsson, T., & Arendt, D. (2014). Larval body patterning and apical organs are conserved in animal evolution. *BMC Biology*, *12*(1), 7. https://doi.org/10.1186/1741-7007-12-7

Martín-Durán, J. M., Pang, K., Børve, A., Lê, H. S., Furu, A., Cannon, J. T., … Hejnol, A. (2018). Convergent evolution of Bilaterian nerve cords. *Nature*, *553*(7686), 45–50. https://doi.org/10.1038/nature25030

Mayer, G., & Harzsch, S. (2007). Immunolocalization of serotonin in Onychophora argues against segmental ganglia being an ancestral feature of arthropods. *BMC Evolutionary Biology*, *7*, 118. https://doi.org/10.1186/1471-2148-7-118

Meyer, N. P., Boyle, M. J., Martindale, M. Q., & Seaver, E. C. (2010). A comprehensive fate map by intracellular injection of identified blastomeres in the marine polychaete *Capitella teleta*. *EvoDevo*, *1*(1), 8. https://doi.org/10.1186/2041-9139-1-8

Meyer, N. P., Carrillo-Baltodano, A., Moore, R. E., & Seaver, E. C. (2015). Nervous system development in lecithotrophic larval and juvenile stages of the annelid *Capitella teleta*. *Frontiers in Zoology*, *12*, 15. https://doi.org/10.1186/s12983-015-0108-y

Meyer, N. P., & Seaver, E. C. (2009). Neurogenesis in an annelid: Characterization of brain neural precursors in the polychaete *Capitella* sp. *I. Developmental Biology*, *335*(1), 237–252. https://doi.org/10.1016/j.ydbio.2009.06.017

Müller, M. C. M. (2006). Polychaete nervous systems: Ground pattern and variations—cLS microscopy and the importance of novel characteristics in phylogenetic analysis. *Integrative and Comparative Biology*, *46*(2), 125–133. https://doi.org/10.1093/icb/icj017

Nomaksteinsky, M., Röttinger, E., Dufour, H., Chettouh, Z., Lowe, C. J., Martindale, M. Q., & Brunet, J.-F. (2009). Centralization of the deuterostome nervous system predates chordates. *Current Biology*, *19*(5), 1264–1269. https://doi.org/10.1016/j.cub.2009.05.063

Orrhage, L., & Müller, M. C. M. (2005). Morphology of the nervous system of Polychaeta (Annelida). *Hydrobiologia*, *535*, 79–111.

Özpolat, B. D., Handberg-thorsager, M., Vervoort, M., & Balavoine, G. (2017). Cell lineage and cell cycling analyses of the 4d micromere using live imaging in the marine annelid *Platynereis dumerilii*. *eLife*, *6* (e30463), 1–35.

Parry, L., Tanner, A., & Vinther, J. (2014). The origin of annelids. *Frontiers in Paleontology*, *57*(6), 1091–1103. https://doi.org/10.1111/pala.12129

Parry, L. A., Edgecombe, G. D., Eibye-jacobsen, D., & Vinther, J. (2016). The impact of fossil data on annelid phylogeny inferred from discrete morphological characters. *Proceedings of the Royal Society. Biological Sciences*, *283*(1837), 20161378.

Pascale, A., Amadio, M., & Quattrone, A. (2008). Defining a neuron: Neuronal ELAV proteins. *Cellular and Molecular Life Sciences*, *65*, 128–140. https://doi.org/10.1007/s00018-007-7017-y

Pavlicek, A., Schwaha, T., & Wanninger, A. (2018). Towards a ground pattern reconstruction of bivalve nervous systems: Neurogenesis in the zebra mussel *Dreissena polymorpha*. *Organisms Diversity & Evolution*, *18* (1), 101–114.

Priyam, A., Woodcroft, B. J., Rai, V., Munagala, A., Moghul, I., & Ter, F. (2015). Sequence server: A modern graphical user interface for custom BLAST databases. *bioRxiv*, *033142*, 1–18.

Prud'homme, B., de Rosa, R., Arendt, D., Julien, J.-F., Pajaziti, R., Dorresteijn, A. W. C., … Balavoine, G. (2003). Arthropod-like expression patterns of *engrailed* and *wingless* in the annelid *Platynereis dumerilii* suggest a role in segment formation. *Current Biology*, *13*(21), 1876–1881. https://doi.org/10.1016/j.cub.2003.10.006

Purschke, G. (2002). On the ground pattern of Annelida. *Organisms Diversity & Evolution*, *2*, 181–196.

Purschke, G. (2016). Annnelida: Basal groups and Pleistoannelida. In A. Schmidt-Rhaesa, S. Harzsch, & G. Purschke (Eds.), *Structure and evolution of invertebrate nervous systems* (pp. 254–312). Oxford, England: Oxford University Press.

Purschke, G., Bleidorn, C., & Struck, T. H. (2014). Systematics, evolution and phylogeny of Annelida—A morphological perspective. *Memoirs of Museum Victoria*, *71*, 247–269.

Ratti, A., Fallini, C., Cova, L., Fantozzi, R., Calzarossa, C., Zennaro, E., … Silani, V. (2006). A role for the ELAV RNA-binding proteins in neural stem cells: Stabilization of *Msi1* mRNA. *Journal of Cell Science*, *119*(7), 1442–1452. https://doi.org/10.1242/jcs.02852

Rawlinson, K. A. (2010). Embryonic and post-embryonic development of the polyclad flatworm *Maritigrella crozieri*; implications for the evolution of spiralian life history traits. *Frontiers in Zoology*, *7*(12), 1–25.

Redl, E., Scherholz, M., Todt, C., Wollesen, T., & Wanninger, A. (2014). Development of the nervous system in Solenogastres (Mollusca) reveals putative ancestral spiralian features. *EvoDevo*, *5*(48), 1–17.

Reuter, M., Wikgren, M., & Lenthonen, M. (1986). Immunocytochemical demonstration of 5HT-like and FMRFamide-like substances in whole mounts of *Microstomum lineare* (Turbellaria). *Cell and Tissue Research*, *246*(1), 7–12.

Rice, M. E. (1973). Morphology, behavior, and histogenesis of the pelagosphera larva of *Phascolosoma agassizii* (Sipuncula). *Smithsoninan Contribution to the Marine Science*, *132*, 1–51.

Rice, M. E. (1985). Sipuncula: Developmental evidence for phylogenetic inference. In S. Morris, J. George, R. Gibson, & H. Platt (Eds.), *The origins and relationships of lower invertebrates* (pp. 274–296). Oxford, England: Oxford University Press.

Rice, M. E. (1993). Sipuncula. In F. W. Harrison & M. E. Rice (Eds.), *Microscopic anatomy of invertebrates Onychophora, Chilopoda, and Lesser Protostomata* (Vol. 12, pp. 274–296). New York, NY: Wiley-Liss.

Richter, S., Loesel, R., Purschke, G., Schmidt-Rhaesa, A., Scholtz, G., Stach, T., … Stegner, M. E. J., S. H. (2010). Invertebrate neurophylogeny: Suggested terms and definitions for a neuroanatomical glossary. *Frontiers in Zoology*, *7*(1), 29. https://doi.org/10.1038/nrg2417. EvoD/Vo

Rimskaya-Korsakova, N., Kristof, A., Malakhov, V. V., & Wanninger, A. (2016). Neural architecture of Galathowenia oculata Zach, 1923 (Oweniidae, Annelida). *Frontiers in Zoology*, *13*(5), 1–19. https://doi.org/10.1186/s12983-016-0136-2

Rizo, J., & Rosenmund, C. (2008). Synaptic vesicle fusion. *Nature Structural & Molecular Biology*, *15*(7), 665–674.

Robinow, S., & White, K. (1991). Characterization and spatial distribution of the ELAV protein during *Drosophila melanogaster* development. *Journal of Neurobiology*, *22*, 443–461.

Rouse, G. W., & Pleijel, F. (2001). *Polychaetes* (1st ed.). Oxford, England: Oxford University Press.

Rousset, V., Pleijel, F., Rouse, G. W., Erséus, C., & Sidall, M. E. (2007). A molecular phylogeny of annelids. *Cladistics*, *23*(1), 41–63.

Samson, M. (2008). Rapid functional diversification in the structurally conserved ELAV family of neuronal RNA binding proteins. *BMC Genomics*, *9*(392), 1–11. https://doi.org/10.1186/1471-2164-9-392

Santagata, S., Resh, C., Hejnol, A., Martindale, M. Q., & Passamaneck, Y. J. (2012). Development of the larval anterior neurogenic domains of *Terebratalia transversa* (Brachiopoda) provides insights into the diversification of larval apical organs and the spiralian nervous system. *EvoDevo*, *3*, 1–20.

Schindelin, J., Arganda-Carreras, I., Frise, E., Kaynig, V., Longair, M., … Cardona, A. (2012). Fiji: an open-source platform for biological-image analysis. *Nature Methods*, *9*, 676–682. https://doi.org/10.1038/nmeth.2019

Schmidt-Rhaesa, A. (2007). *The evolution of organ systems*. Oxford, England: Oxford University Press.

Scholtz, G. (2002). The Articulata hypothesis–or what is a segment? *Organisms Diversity & Evolution*, *2*(3), 197–215. https://doi.org/10.1078/1439-6092-00046

Schulze, A., Cutler, E. B., & Giribet, G. (2005). Reconstructing they phylogeny of the Sipuncula. *Hydrobiologia*, *535/536*, 277–296. https://doi.org/10.1007/s10750-004-4404-3

Seaver, E. C. (2003). Segmentation: Mono- or polyphyletic? *International Journal of Developmental Biology*, *47*(7–8), 583–595. Retrieved from. http://www.ncbi.nlm.nih.gov/pubmed/14756334

Seaver, E. C., & Kaneshige, L. M. (2006). Expression of "segmentation" genes during larval and juvenile development in the polychaetes *Capitella* sp. I and H. elegans. *Developmental Biology*, *289*(1), 179–194. https://doi.org/10.1016/j.ydbio.2005.10.025

Seaver, E. C., Paulson, D. a., Irvine, S. Q., & Martindale, M. Q. (2001). The spatial and temporal expression of Ch-en, the engrailed gene in the polychaete *Chaetopterus*, does not support a role in body axis segmentation. *Developmental Biology*, *236*(1), 195–209. https://doi.org/10.1006/dbio.2001.0309

Seaver, E. C., Thamm, K., & Hill, S. D. (2005). Growth patterns during segmentation in the two polychaete annelids, *Capitella* sp. I and *Hydroides elegans*: Comparisons at distinct life history stages. *Evolution & Development*, *7*(4), 312–326. https://doi.org/10.1111/j.1525-142X.2005.05037.x

Shigeno, S., Parnaik, R., Albertin, C. B., & Ragsdale, C. W. (2015). Evidence for a cordal, not ganglionic, pattern of cephalopod brain neurogenesis. *Zoological Letters*, *1*(26), 1–13. https://doi.org/10.1186/s40851-015-0026-z

Simionato, E., Kerner, P., Dray, N., Le Gouar, M., Ledent, V., Arendt, D., & Vervoort, M. (2008). Atonal- and achaete-scute-related genes in the annelid *Platynereis dumerilii*: Insights into the evolution of neural basic-helix-loop-helix genes. *BMC Evolutionary Biology*, *8*, 170. https://doi.org/10.1186/1471-2148-8-170

Sperling, E. A., Vinther, J., Moy, V. N., Wheeler, B. M., Sémon, M., Briggs, D. E. G., & Peterson, K. J. (2009). MicroRNAs resolve an apparent conflict between annelid systematics and their fossil records. *Proceedings of the Royal Society B*, *276*, 4315–4322. https://doi.org/10.1098/rspb.2009.1340

Starunov, V. V., Voronezhskaya, E. E., & Nezlin, L. P. (2017). Development of the nervous system in Platynereis dumerilii (Nereididae, Annelida). *Frontiers in Zoology*, *14*(27), 1–20. https://doi.org/10.1186/s12983-017-0211-3

Steinmetz, P. R. H., Kostyuchenko, R. P., Fischer, A., & Arendt, D. (2011). The segmental pattern of *otx*, *gbx*, and *Hox* genes in the annelid *Platynereis dumerilii*. *Evolution & Development*, *13*(1), 72–79. https://doi.org/10.1111/j.1525-142X.2010.00457.x

Stephen, A. C., & Edmonds, S. J. (1972). *They phyla Sipuncula and Echiura*. London, England: British Museum.

Struck, T. H., Golombek, A., Weigert, A., Franke, F. A., Westheide, W., Purschke, G., … Halanych, K. M. (2015). The evolution of annelids reveals two adaptive routes to the interstitial realm. *Current Biology*, *25*(15), 1993–1999. https://doi.org/10.1016/j.cub.2015.06.007

Struck, T. H., Paul, C., Hill, N., Hartmann, S., Hösel, C., Kube, M., … Bleidorn, C. (2011). Phylogenomic analyses unravel annelid evolution. *Nature*, *471*(7336), 95–98. https://doi.org/10.1038/nature09864

Struck, T. H., Schult, N., Kusen, T., Hickman, E., Bleidorn, C., McHugh, D., & Halanych, K. M. (2007). Annelid phylogeny and the status of Sipuncula and Echiura. *BMC Evolutionary Biology*, *7*, 57. https://doi.org/10.1186/1471-2148-7-57

Sur, A., Magie, C. R., Seaver, E. C., & Meyer, N. P. (2017). Spatiotemporal regulation of nervous system development in the annelid *Capitella teleta*. *EvoDevo*, *8*, 1–23. https://doi.org/10.1186/s13227-017-0076-8

Thamm, K., & Seaver, E. C. (2008). Notch signaling during larval and juvenile development in the polychaete annelid *Capitella* sp. I. *Developmental Biology*, *320*(1), 304–318. https://doi.org/10.1016/j.ydbio.2008.04.015

Verasztó, C., Gühmann, M., Jia, H., Rajan, V. B. V., Bezares-Calderón, L. A., Piñeiro-López, C., … Jékely, G. (2018). Ciliary and rhabdomeric photoreceptor-cell circuits form a spectral depth gauge in marine zooplankton. *eLife*, *7*(e36440), 1–19.

Verasztó, C., Ueda, N., Bezares-Calderón, L. A., Panzera, A., Williams, E. A., Shadidi, R., & Jékely, G. (2017). Ciliomotor circuitry underlying whole-body coordination of ciliary activity in the *Platynereis* larva. *eLife*, *6*, e26000. https://doi.org/10.7554/eLife.26000

von Mack, H. (1902). Das Centralnervensystem Von *Sipunculus nudus* L. (Bulchstrang). Mitt Besonderer Berucksightigung Untersuchung. *Arbeiten Aus Dem Zoologischen Instituten Der Universität Wien Und Der Zoologischen Station in Triest*, *13*, 237–334.

Voronezhskaya, E. E., Tyurin, S. A., & Nezlin, L. P. (2002). Neuronal development in larval chiton *Ischnochiton hakodadensis* (Mollusca: Polyplacophora). *The Journal of Comparative Neurology*, *38*, 25–38. https://doi.org/10.1002/cne.10130

Wakamatsu, Y., & Weston, J. (1997). Sequential expression and role of Hu RNA-binding proteins during neurogenesis. *Development*, *124*, 3349–3460.

Wanninger, A. (2008). Comparative lophotrochozoan neurogenesis and larval neuroanatomy: Recent advances from previously neglected taxa. *Acta Biologica Hungarica*, *59*, 127–136. https://doi.org/10.1556/ABiol.59.2008.Suppl.21

Wanninger, A., & Haszprunar, G. (2003). The development of the serotonergic and FMRF-amidergic nervous system in *Antalis entalis* (Mollusca, Scaphopoda). *Zoomorphology*, *122*, 77–85. https://doi.org/10.1007/s00435-003-0071-6

Wanninger, A., Koop, D., Bromham, L., Noonan, E., & Degnan, B. M. (2005). Nervous and muscle system development in *Phascolion strombus* (Sipuncula). *Development Genes and Evolution*, *215*(10), 509–518. https://doi.org/10.1007/s00427-005-0012-0

Weigert, A., & Bleidorn, C. (2016). Current status of annelid phylogeny. *Organisms Diversity & Evolution*, *16*(2), 345–362. https://doi.org/10.1007/s13127-016-0265-7

Weigert, A., Helm, C., Meyer, M., Nickel, B., Arendt, D., Hausdorf, B., … Struck, T. H. (2014). Illuminating the base of the annelid tree using transcriptomics. *Molecular Biology and Evolution*, *31*(6), 1391–1401. https://doi.org/10.1093/molbev/msu080

Young, C. M., Sewell, M. A., & Rice, M. E. (2002). *Atlas of marine invertebrates larvae* (1st ed.), Cambridge, MA: Academic Press.

Yurchenko, O. V., Skiteva, O. I., Voronezhskaya, E. E., & Dyachuk, V. A. (2018). Nervous system development in the Pacific oyster, *Crassostrea gigas* (Mollusca: Bivalvia). *Frontiers in Zoology*, *15*(10), 1–21.

Zattara, E. E., & Bely, A. E. (2015). Fine taxonomic sampling of nervous systems within Naididae (Annelida: Clitellata) reveals evolutionary lability and revised homologies of annelid neural components. *Frontiers in Zoology*, *12*(8), 1–21. https://doi.org/10.1186/s12983-015-0100-6

Zrzavý, J., Pavel, Ř., Piálek, L., & Janouškovec, J. (2009). Phylogeny of Annelida (Lophotrochozoa): Total-evidence analysis of morphology and six genes. *BMC Evolutionary Biology*, *9*(189), 1–14. https://doi.org/10.1186/1471-2148-9-189

SUPPORTING INFORMATION

Additional supporting information may be found online in the Supporting Information section at the end of this article.

How to cite this article: Carrillo-Baltodano AM, Boyle MJ, Rice ME, Meyer NP. Developmental architecture of the nervous system in *Themiste lageniformis* (Sipuncula): New evidence from confocal laser scanning microscopy and gene expression. *Journal of Morphology*. 2019;1–23. https://doi.org/10.1002/jmor.21054